CHAPTER

12

Bioelectric Phenomena

John D. Enderle, PhD

OUTLINE

AT THE CONCLUSION OF THIS CHAPTER, STUDENTS WILL BE ABLE TO:

- Describe the history of bioelectric phenomenon.
- Qualitatively explain how signaling occurs among neurons.
- Calculate the membrane potential due to one or more ions.
- Compute the change in membrane potential due to a current pulse through a cell membrane.
- Describe the change in membrane potential with distance after stimulation.
- Explain the voltage clamp experiment and an action potential.
- Simulate an action potential using the Hodgkin-Huxley model.
- Describe the process used for communication among neurons.

12.1 INTRODUCTION

Chapter 3 briefly described the nervous system and the concept of a neuron. Here, the description of a neuron is extended by examining its properties at rest and during excitation. The concepts introduced here are basic and allow further investigation of more sophisticated models of the neuron or groups of neurons by using GENESIS (a general neural simulation program; see suggested reading by J.M. Bower and D. Beeman) or extensions of the Hodgkin-Huxley model by using more accurate ion channel descriptions and neural networks. The models introduced here are an important first step in understanding the nervous system and how it functions.

Models of the neuron presented in this chapter have a rich history of development. This history continues today as new discoveries unfold that supplant existing theories and models. Much of the physiological interest in models of a neuron involves the neuron's use in transferring and storing information, while much engineering interest involves the neuron's use as a template in computer architecture and neural networks. New developments in brain-machine interfacing make understanding the neuron even more important today (see [4] and [1] for additional information). To fully appreciate the operation of a neuron, it is important to understand the properties of a membrane at rest by using standard biophysics, biochemistry, and electric circuit tools. In this way, a more qualitative awareness of signaling via the generation of the action potential can be better understood.

The Hodgkin and Huxley theory that was published in 1952 described a series of experiments that allowed the development of a model of the action potential. This work was awarded a Nobel Prize in 1963 (shared with John Eccles) and is covered in Section 12.6. It is reasonable to question the usefulness of covering the Hodgkin-Huxley model in a textbook today, given all of the advances since 1952. One simple answer is that this model is one of the few timeless classics and should be covered. Another is that all current, and perhaps future, models have their roots in this model.

Section 12.2 describes a brief history of bioelectricity and can be easily omitted on first reading of the chapter. Section 12.3 describes the structure and provides a qualitative description of a neuron. Biophysics and biochemical tools that are useful in understanding the properties of a neuron at rest are presented in Section 12.4. An equivalent circuit model of a cell membrane at rest consisting of resistors, capacitors, and voltage sources is described in Section 12.5. Section 12.6 describes the Hodgkin-Huxley model of a neuron and includes a brief description of their experiments and the mathematical model describing an action potential. Finally, Section 12.7 provides a model of the whole neuron.

12.2 HISTORY

12.2.1 The Evolution of a Discipline: The Galvani-Volta Controversy

In 1791, an article appeared in the Proceedings of the Bologna Academy, reporting experimental results that, it was claimed, proved the existence of animal electricity. This now famous publication was the work of Luigi Galvani. At the time of its publication, this article caused a great deal of excitement in the scientific community and sparked

a controversy that ultimately resulted in the creation of two separate and distinct disciplines: electrophysiology and electrical engineering. The controversy arose from the different interpretations of the data presented in this now famous article. Galvani was convinced that the muscular contractions he observed in frog legs were due to some form of electrical energy emanating from the animal. On the other hand, Allesandro Volta, a professor of physics at the University of Padua, was convinced that the "electricity" described in Galvani's experiments originated not from the animal but from the presence of the dissimilar metals used in Galvani's experiments. Both of these interpretations were important. The purpose of this section, therefore, is to discuss them in some detail, highlighting the body of scientific knowledge available at the time these experiments were performed, the rationale behind the interpretations that were formed, and their ultimate effect.

12.2.2 Electricity in the Eighteenth Century

Before 1800, a considerable inventory of facts relating to electricity in general and bioelectricity in particular had accumulated. The Egyptians and Greeks had known that certain fish could deliver substantial shocks to an organism in their aqueous environment. Static electricity had been discovered by the Greeks, who produced it by rubbing resin (amber or, in Greek, *elektron*) with cat's fur or by rubbing glass with silk. For example, Thales of Miletus reported in 600 BC that a piece of amber when vigorously rubbed with a cloth responded with an "attractive power." Light particles such as chaff, bits of papyrus, and thread jumped to the amber from a distance and were held to it. The production of static electricity at that time became associated with an aura.

More than two thousand years elapsed before the English physician William Gilbert picked up where Thales left off. Gilbert showed that not only amber but also glass, agate, diamond, sapphire, and many other materials when rubbed exhibited the same attractive power described by the Greeks. However, Gilbert did not report that particles could also be repelled. It was not until a century later that electrostatic repulsion was noted by Charles DuFay (1698–1739) in France.

The next step in the progress of electrification was an improvement of the friction process. Rotating rubbing machines were developed to give continuous and large-scale production of electrostatic charges. The first of these frictional electric machines was developed by Otto von Guericke (1602–1685) in Germany. In the eighteenth century, electrification became a popular science, and experimenters discovered many new attributes of electrical behavior. In England, Stephen Gray (1666–1736) proved that electrification could flow hundreds of feet through ordinary twine when suspended by silk threads. Thus, he theorized that electrification was a "fluid." Substituting metal wires for the support threads, he found that the charges would quickly dissipate. Thus, the understanding that different materials can either conduct or insulate began to take shape. The "electrics," like silk, glass, and resin, held charge. The "nonelectrics," like metals and water, conducted charges. Gray also found that electrification could be transferred by proximity of one charged body to another without direct contact. This was evidence of electrification by induction, a principle that was used later in machines that produced electrostatic charges.

In France, Charles F. DuFay, a member of the French Academy of Science, was intrigued by Gray's experiments. DuFay showed by extensive tests that practically all materials, with the exception of metals and those too soft or fluid to be rubbed, could be electrified. Later, however, he discovered that if metals were insulated, they could hold the largest electric charge of all. DuFay found that rubbed glass would repel a piece of gold leaf, whereas rubbed amber, gum, or wax attracted it. He concluded that there were two different kinds of electric "fluids," which he labeled "vitreous" and "resinous." He found that while unlike charges attracted each other, like charges repelled. This indicated that there were two kinds of electricity.

In the American colonies, Benjamin Franklin (1706–1790) became interested in electricity and performed experiments that led to his hypothesis regarding the "one-fluid theory." Franklin stated that there was only one type of electricity and that the electrical effects produced by friction reflected the separation of electric fluid so one body contained an excess and the other a deficit. He argued that "electrical fire" is a common element in all bodies and is normally in a balanced or neutral state. Excess or deficiency of charge, such as that produced by the friction between materials, created an imbalance. Electrification by friction was, thus, a process of separation rather than a creation of charge. By balancing a charge gain with an equal charge loss, Franklin had implied a law—namely, that the quantity of the electric charge is conserved. Franklin guessed that when glass was rubbed, the excess charge appeared on the glass, and he called that "positive" electricity. He thus established the direction of conventional current from positive to negative. It is now known that the electrons producing a current move in the opposite direction.

Out of this experimental activity came an underlying philosophy or law. Up to the end of the eighteenth century, the knowledge of electrostatics was mainly qualitative. There were means for detecting but not for measuring, and the relationships between the charges had not been formulated. The next step was to quantify the phenomena of electrostatic charge forces.

For this determination, the scientific scene shifted back to France and the engineer-turned-physicist Charles A. Coulomb (1726–1806). Coulomb demonstrated that a force is exerted when two charged particles are placed in the vicinity of each other. However, he went a step beyond experimental observation by deriving a general relationship that completely expressed the magnitude of this force. His inverse-square law for the force of attraction or repulsion between charged bodies became one of the major building blocks in understanding the effect of a fundamental property of matter-charge. However, despite this wide array of discoveries, it is important to note that before the time of Galvani and Volta, there was no source that could deliver a continuous flow of electric fluid, a term that we now know implies both charge and current.

In addition to a career as statesman, diplomat, publisher, and signer of both the Declaration of Independence and the Constitution, Franklin was an avid experimenter and inventor. In 1743 at the age of 37, Franklin witnessed with excited interest a demonstration of static electricity in Boston and resolved to pursue the strange effects with investigations of his own. Purchasing and devising various apparati, Franklin became an avid electrical enthusiast. He launched into many years of experiments with electrostatic effects.

Franklin, the scientist, is most popularly known for his kite experiment during a thunderstorm in June 1752 in Philadelphia. Although various European investigators had surmised the identity of electricity and lightning, Franklin was the first to prove by an experimental procedure and demonstration that lightning was a giant electrical spark. Having previously noted the advantages of sharp metal points for drawing "electrical fire," Franklin put them to use as "lightning rods." Mounted vertically on rooftops, they would dissipate the thundercloud charge gradually and harmlessly to the ground. This was the first practical application in electrostatics.

Franklin's work was well received by the Royal Society in London. The origin of such noteworthy output from remote and colonial America made Franklin especially marked. In his many trips to Europe as statesman and experimenter, Franklin was lionized in social circles and eminently regarded by scientists.

12.2.3 Galvani's Experiments

Against such a background of knowledge of the "electric fluid" and the many powerful demonstrations of its ability to activate muscles and nerves, it is readily understandable that biologists began to suspect that the "nervous fluid" or the "animal spirit" postulated by Galen to course in the hollow cavities of the nerves and mediate muscular contraction, and indeed all the nervous functions, was of an electrical nature. Galvani, an obstetrician and anatomist, was by no means the first to hold such a view, but his experimental search for evidence of the identity of the electric and nervous fluids provided the critical breakthrough.

Speculations that the muscular contractions in the body might be explained by some form of animal electricity were common. By the eighteenth century, experimenters were familiar with the muscular spasms of humans and animals that were subjected to the discharge of electrostatic machines. As a result, electric shock was viewed as a muscular stimulant. In searching for an explanation of the resulting muscular contractions, various anatomical experiments were conducted to study the possible relationship of "metallic contact" to the functioning of animal tissue. In 1750, Johann Sulzer (1720–1779), a professor of physiology at Zurich, described a chance discovery that an unpleasant acid taste occurred when the tongue was put between two strips of different metals, such as zinc and copper, whose ends were in contact. With the metallic ends separated, there was no such sensation. Sulzer ascribed the taste phenomenon to a vibratory motion set up in the metals that stimulated the tongue and used other metals with the same results. However, Sulzer's reports went unheeded for a half-century until new developments called attention to his findings.

The next fortuitous and remarkable discovery was made by Luigi Galvani (1737–1798), a descendant of a very large Bologna family, who at age 25 was made Professor of Anatomy at the University of Bologna. Galvani had developed an ardent interest in electricity and its possible relation to the activity of the muscles and nerves. Dissected frog legs were convenient specimens for investigation, and in his laboratory Galvani used them for studies of muscular and nerve activity. In these experiments, he and his associates were studying the responses of the animal tissue to various stimulations. In this setting, Galvani observed that while a freshly prepared frog leg was being probed by a scalpel, the leg jerked

convulsively whenever a nearby frictional electrical machine gave off sparks. Galvani said the following of his experiments:

> I had dissected and prepared a frog, and laid it on a table, on which there was an electrical machine. It so happened by chance that one of my assistants touched the point of his scalpel to the inner crural nerve of the frog; the muscles of the limb were suddenly and violently convulsed. Another of those who were helping to make the experiments in electricity thought that he noticed this happening only at the instant a spark came from the electrical machine. He was struck with the novelty of the action. I was occupied with other things at the time, but when he drew my attention to it, I immediately repeated the experiment. I touched the other end of the crural nerve with the point of my scalpel, while my assistant drew sparks from the electrical machine. At each moment when sparks occurred, the muscle was seized with convulsions.

With an alert and trained mind, Galvani designed an extended series of experiments to resolve the cause of the mystifying muscle behavior. On repeating the experiments, he found that touching the muscle with a metallic object while the specimen lay on a metal plate provided the condition that resulted in the contractions.

Having heard of Franklin's experimental proof that a flash of lightning was of the same nature as the electricity generated by electric machines, Galvani set out to determine whether atmospheric electricity might produce the same results observed with his electrical machine. By attaching the nerves of frog legs to aerial wires and the feet to another electrical reference point known as an electrical ground, he noted the same muscular response during a thunderstorm that he observed with the electrical machine. It was another chance observation during this experiment that lead to further inquiry, discovery, and controversy.

Galvani also noticed that the prepared frogs, which were suspended by brass hooks through the marrow and rested against an iron trellis, showed occasional convulsions regardless of the weather. In adjusting the specimens, he pressed the brass hook against the trellis and saw the familiar muscle jerk occurring each time he completed the metallic contact. To check whether this jerking might still be from some atmospheric effect, he repeated the experiment inside the laboratory. He found that the specimen, laid on an iron plate, convulsed each time the brass hook in the spinal marrow touched the iron plate. Recognizing that some new principle was involved, he varied his experiments to find the true cause. In the process, he found that by substituting glass for the iron plate, the muscle response was not observed, but using a silver plate restored the muscle reaction. He then joined equal lengths of two different metals and bent them into an arc. When the tips of this bimetallic arc touched the frog specimens, the familiar muscular convulsions were obtained. As a result, he concluded not only that metal contact was a contributing factor but also that the intensity of the convulsion varied according to the kinds of metals joined in the arc pair.

Galvani was now faced with trying to explain the phenomena he was observing. He had encountered two electrical effects for which his specimens served as indicator: one from the sparks of the electrical machine and the other from the contact of dissimilar metals. Either the electricity responsible for the action resided in the anatomy of the specimens with the metals serving to release it or the effect was produced by the bimetallic contact, with the specimen serving only as an indicator.

Galvani was primarily an anatomist and seized on the first explanation. He ascribed the results to "animal electricity" that resided in the muscles and nerves of the organism itself.

Using a physiological model, he compared the body to a Leyden jar, in which the various tissues developed opposite electrical charges. These charges flowed from the brain through nerves to the muscles. Release of electrical charge by metallic contact caused the convulsions of the muscles. "The idea grew," he wrote, "that in the animal itself there was indwelling electricity. We were strengthened in such a supposition by the assumption of a very fine nervous fluid that during the phenomena flowed into the muscle from the nerve, similar to the electric current of a Leyden jar." Galvani's hypothesis reflected the prevailing view of his day that ascribed the body activation to a flow of "spirits" residing in the various body parts.

In 1791, Galvani published his paper *De Viribus Electricitatis In Motu Musculari* in the Proceedings of the Academy of Science in Bologna. This paper set forth his experiments and conclusions. Galvani's report created a sensation and implied to many a possible revelation of the mystery of the life force. Men of science and laymen alike, both in Italy and elsewhere in Europe, were fascinated and challenged by these findings. However, no one pursued Galvani's findings more assiduously and used them as a stepping stone to greater discovery than Allesandro Volta.

12.2.4 Volta's Interpretation

Galvani's investigations aroused a virtual furor of interest. Wherever frogs were found, scientists repeated his experiments with routine success. Initially, Galvani's explanation for the muscular contractions was accepted without question—even by the prominent physician Allesandro Volta, who had received a copy of Galvani's paper and verified the phenomenon.

Volta was a respected scientist in his own right. At age 24, Volta published his first scientific paper, *On the Attractive Force of the Electric Fire*, in which he speculated about the similarities between electric force and gravity. Engaged in studies of physics and mathematics and busy with experimentation, Volta's talents were so evident that before the age of 30 he was named the Professor of Physics at the Royal School of Como. Here he made his first important contribution to science with the invention of the electrophorus or "bearer of electricity." This was the first device to provide a replenishable supply of electric charge by induction rather than by friction.

In 1782, Volta was called to the professorship of physics at the University of Padua. There he made his next invention, the condensing electrophorus, a sensitive instrument for detecting electric charge. Earlier methods of charge detection employed the "electroscope," which consisted of an insulated metal rod that had pairs of silk threads, pith balls, or gold foil suspended at one end. These pairs diverged by repulsion when the rod was touched by a charge. The amount of divergence indicated the strength of the charge and thus provided quantitative evidence for Coulomb's Law.

By combining the electroscope with his electrophorus, Volta provided the scientific community with a detector for minute quantities of electricity. Volta continued to innovate and made his condensing electroscope a part of a mechanical balance that made it possible to measure the force of an electric charge against the force of gravity. This instrument was called an electrometer and was of great value in Volta's later investigations of the electricity created by contact of dissimilar metals.

Volta expressed immediate interest on learning of Galvani's 1791 report to the Bologna Academy on the "Forces of Electricity in Their Relation to Muscular Motion." Volta set out quickly to repeat Galvani's experiments and initially confirmed Galvani's conclusions on "animal electricity" as the cause of the muscular reactions. Along with Galvani, he ascribed the activity to an imbalance between electricity of the muscle and that of the nerve, which was restored to equilibrium when a metallic connection was made. On continuing his investigations, however, Volta began to have doubts about the correctness of that view. He found inconsistencies in the balance theory. In his experiments, muscles would convulse only when the nerve was in the electrical circuit made by metallic contact.

In an effort to find the true cause of the observed muscle activity, Volta went back to an experiment previously performed by Sulzer. When Volta placed a piece of tinfoil on the tip and a silver coin at the rear of his tongue and connected the two with a copper wire, he got a sour taste. When he substituted a silver spoon for the coin and omitted the copper wire, he got the same result as when he let the handle of the spoon touch the foil. When using dissimilar metals to make contact between the tongue and the forehead, he got a sensation of light. From these results, Volta came to the conclusion that the sensations he experienced could not originate from the metals as conductors but must come from the ability of the dissimilar metals themselves to generate electricity.

After two years of experimenting, Volta published his conclusions in 1792. While crediting Galvani with a surprising original discovery, he disagreed with him on what produced the effects. By 1794, Volta had made a complete break with Galvani. He became an outspoken opponent of the theory of animal electricity and proposed the theory of "metallic electricity." Galvani, by nature a modest individual, avoided any direct confrontation with Volta on the issue and simply retired to his experiments on animals.

Volta's conclusive demonstration that Galvani had not discovered animal electricity was a blow from which the latter never recovered. Nevertheless, he persisted in his belief in animal electricity and conducted his third experiment, which definitely proved the existence of bioelectricity. In this experiment, he held one foot of the frog nerve-muscle preparation and swung it so the vertebral column and the sciatic nerve touched the muscles of the other leg. When this occurred or when the vertebral column was made to fall on the thigh, the muscles contracted vigorously. According to most historians, it was his nephew Giovanni Aldini (1762–1834) who championed Galvani's cause by describing this important experiment in which he probably collaborated. The experiment conclusively showed that muscular contractions could be evoked without metallic conductors. According to Fulton and Cushing, Aldini wrote:

> Some philosophers, indeed, had conceived the idea of producing contractions in a frog without metals; and ingenious methods, proposed by my uncle Galvani, induced me to pay attention to the subject, in order that I might attain to greater simplicity. He made me sensible of the importance of the experiment and therefore I was long ago inspired with a desire of discovering that interesting process. It will be seen in the Opuscoli of Milan (No. 21) that I showed publicly, to the Institute of Bologna, contractions in a frog without the aid of metals so far back as the year 1794. The experiment, as described in a memoir addressed to M. Amorotti [*sic*] is as follows: I immersed a prepared frog in a strong solution of muriate of soda. I then took it from the solution, and, holding one extremity of it in my hand, I suffered the other to hang freely down. While in this position, I raised up the nerves with a small glass rod, in such a manner that they did not touch the muscles. I then suddenly removed the glass rod, and every time that the spinal marrow

> and nerves touched the muscular parts, contractions were excited. Any idea of a stimulus arising earlier from the action of the salt, or from the impulse produced by the fall of the nerves, may be easily removed. Nothing will be necessary but to apply the same nerves to the muscles of another prepared frog, not in a Galvanic circle; for, in this case, neither the salt, nor the impulse even if more violent, will produce muscular motion.

The claims and counterclaims of Volta and Galvani developed rival camps of supporters and detractors. Scientists swayed from one side to the other in their opinions and loyalties. Although the subject was complex and not well understood, it was on the verge of an era of revelation. The next great contribution to the field was made by Carlo Matteucci, who both confirmed Galvani's third experiment and made a new discovery. Matteucci showed that the action potential precedes the contraction of skeletal muscle. In confirming Galvani's third experiment, which demonstrated the injury potential, Matteucci noted:

> I injure the muscles of any living animal whatever, and into the interior of the wound I insert the nerve of the leg, which I hold, insulated with glass tube. As I move this nervous filament in the interior of the wound, I see immediately strong contractions in the leg. To always obtain them, it is necessary that one point of the nervous filament touches the depths of the wound, and that another point of the same nerve touches the edge of the wound.

By using a galvanometer, Matteucci found that the difference in potential between an injured and uninjured area was diminished during a tetanic contraction. The study of this phenomenon occupied the attention of all succeeding electrophysiologists. More than this, however, Matteucci made another remarkable discovery: that a transient bioelectric event, now designated the action potential, accompanies the contraction of intact skeletal muscle. He demonstrated this by showing that a contracting muscle is able to stimulate a nerve that, in turn, causes contraction of the muscle it innervates. The existence of a bioelectric potential was established through the experiments of Galvani and Matteucci. Soon thereafter, the presence of an action potential was discovered in cardiac muscle and nerves.

Volta, on the other hand, advocated that the source of the electricity was due to the contact of the dissimilar metals only, with the animal tissue acting merely as the indicator. His results differed substantially depending on the pairs of metals used. For example, Volta found that the muscular reaction from dissimilar metals increased in vigor depending on the metals that were used.

In an effort to obtain better quantitative measurements, Volta dispensed with the use of muscles and nerves as indicators. He substituted instead his "condensing electroscope." He was fortunate in the availability of this superior instrument because the contact charge potential of the dissimilar metals was minute, far too small to be detected by the ordinary gold-leaf electroscope. Volta's condensing electroscope used a stationary disk and a removable disk separated by a thin insulating layer of shellac varnish. The thinness of this layer provided a large capacity for accumulation of charge. When the upper disk was raised after being charged, the condenser capacity was released to give a large deflection of the gold leaves.

Volta proceeded systematically to test the dissimilar metal contacts. He made disks of various metals and measured the quantity of the charge on each disk combination by the divergence of his gold foil condensing electroscope. He then determined whether the charge was positive or negative by bringing a rubbed rod of glass or resin near the electroscope. The effect of the rod on the divergence of the gold foil indicated the polarity of the charge.

Volta's experiments led him toward the idea of an electric force or electrical "potential." This, he assumed, resided in contact between the dissimilar metals. As Volta experimented with additional combinations, he found that an electrical potential also existed when there was contact between the metals and some fluids. As a result, Volta added liquids, such as brine and dilute acids, to his conducting system and classified the metal contacts as "electrifiers of the first class" and the liquids as electrifiers of the "second class."

Volta found that there was only momentary movement of electricity in a circuit composed entirely of dissimilar metals. However, when he put two dissimilar metals in contact with a separator soaked with a saline or acidified solution, there was a steady indication of potential. In essence, Volta was assembling the basic elements of an electric battery: two dissimilar metals and a liquid separator. Furthermore, he found that the overall electric effect could be enlarged by multiplying the elements. Thus, by stacking metal disks and the moistened separators vertically, he constructed an "electric pile," the first electric battery. This was the most practical discovery of his career.

12.2.5 The Final Result

Considerable time passed before true explanations became available for what Galvani and Volta had done. Clearly, both demonstrated the existence of a difference in electric potential, but what had produced it eluded them. The potential difference present in the experiments carried out by both investigators is now clearly understood. Although Galvani thought that he had initiated muscular contractions by discharging animal electricity resident in a physiological capacitor consisting of the nerve (inner conductor) and muscle surface (outer conductor), it is now known that the stimulus consists of an action potential that in turn causes muscular contractions.

It is interesting to note that the fundamental unit of the nervous system—the neuron—has an electric potential between the inside and outside of the cell, even at rest. This membrane-resting potential is continually affected by various inputs to the cell. When a certain potential is reached, an action potential is generated along its axon to all of its distant connections. This process underlies the communication mechanisms of the nervous system. Volta's discovery of the electrical battery provided the scientific community with the first steady source of electrical potential, which when connected in an electric circuit consisting of conducting materials or liquids, results in the flow of electrical charge—that is, electrical current. This device launched the field of electrical engineering.

12.3 NEURONS

A reasonable estimate of the human brain is that it contains about 10^{12} neurons partitioned into fewer than 1,000 different types in an organized structure of rather uniform appearance. While not important in this chapter, it is important to note that there are two classes of neuron: the nerve cell and the neuroglial cell. Even though there are 10 to 50 times as many neuroglial cells as nerve cells in the brain, attention is focused here on the nerve cell, since the neuroglial cells are not involved in signaling and primarily provide a support function for the nerve cell. Therefore, the terms *neuron* and *nerve cell* are used interchangeably,

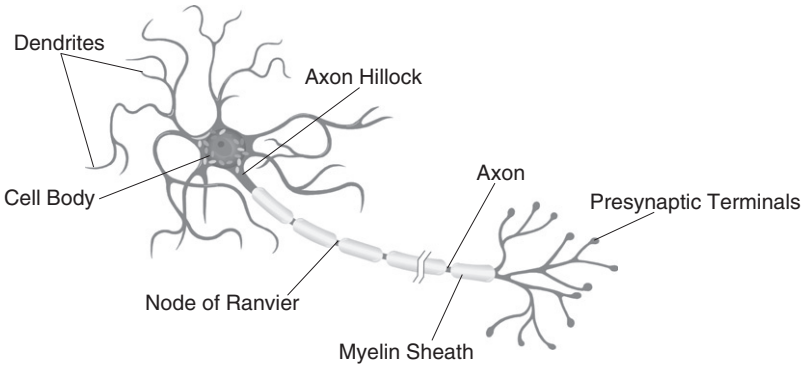

FIGURE 12.1 A typical neuron.

since the primary focus here is to better understand the signaling properties of a neuron. Overall, the complex abilities of the brain are best described by virtue of a neuron's interconnections with other neurons or the periphery and not a function of the individual differences among neurons.

A typical neuron, as shown in Figure 12.1, is defined with four major regions: cell body (also referred to as the soma), dendrites, axon, and presynaptic terminals. The cell body of a neuron contains the nucleus and other organelles needed to nourish the cell and is similar to other cells. Unlike other cells, however, the neuron's cell body is connected to a number of branches called dendrites and a long tube called the axon that connects the cell body to the presynaptic terminals. Some neurons have multiple axons.

Dendrites are the receptive surfaces of the neuron that receive signals from thousands of other neurons passively and without amplification. Located on the dendrite and cell body are receptor sites that receive input from presynaptic terminals from adjacent neurons. Neurons typically have 10^4 to 10^5 synapses. Communication between neurons is through chemical synapses. Chemical synapses, as described in Chapter 3, involve the use of a neurotransmitter that changes the membrane potential of an adjacent neuron. Other cells, such as muscle and cardiac cells, use electrical synapses. An electrical synapse involves the use of a gap junction that directly connects the two cells together through a pore.

Also connected to the neuron cell body is a single axon that ranges in length from 1 meter in the human spinal cord to a few millimeters in the brain. The diameter of the axon also varies from less than 1 to 500 μm. In general, the larger the diameter of the axon, the faster the signal travels. Signals traveling in the axon range from 0.5 m/s to 120 m/s. The purpose of an axon is to serve as a transmission line to move information from one neuron to another at great speeds. Some axons are surrounded by a fatty insulating material called the myelin sheath and have regular gaps, called the nodes of Ranvier, that allow the action potential to jump from one node to the next. The action potential is most easily envisioned as a pulse that travels the length of the axon without decreasing in amplitude.

Most of the remainder of this chapter is devoted to understanding this process. At the end of the axon is a network of up to 10,000 branches with endings called the presynaptic terminals. A diagram of the presynaptic terminal is shown in Figure 3.28. All action potentials that

move through the axon propagate through each branch to the presynaptic terminal. The presynaptic terminals are the transmitting units of the neuron, which, when stimulated, release a neurotransmitter that flows across a gap of approximately 20 nanometers to an adjacent cell, where it interacts with the postsynaptic membrane and changes its potential.

12.3.1 Membrane Potentials

The neuron, like other cells in the body, has a separation of charge across its external membrane. The cell membrane is positively charged on the outside and negatively charged on the inside, as illustrated in Figure 12.2. This separation of charge, due to the selective permeability of the membrane to ions, is responsible for the membrane potential. In the neuron, the potential difference across the cell membrane is approximately 60 mV to 90 mV, depending on the specific cell. By convention, the outside is defined as 0 mV (ground), and the resting potential is $V_m = v_i - v_o = -60$ mV. This charge differential is of particular interest, since most signaling involves changes in this potential across the membrane. Signals such as action potentials are a result of electrical perturbations of the membrane. By definition, if the membrane is more negative than resting potential (i.e., -60 to -70 mV), it is called *hyperpolarization*, and an increase in membrane potential from resting potential (i.e., -60 to -50 mV) is called *depolarization*. As described later, ions travel across the cell membrane through ion selective channels.

Creating a membrane potential of -60 mV does not require the separation of many positive and negative charges across the membrane. The actual number, however, can be found from the relationship $Cdv = dq$, or $C\Delta v = \Delta q$ (Δq = the number of charges times the electron charge of 1.6022×10^{-19}C). Therefore, with $C = 1\ \mu F/cm^2$ and $\Delta v = 60 \times 10^{-3}$, the number of charges equals approximately 1×10^8 per cm^2. These charges are located within a distance of 1 μm from the membrane.

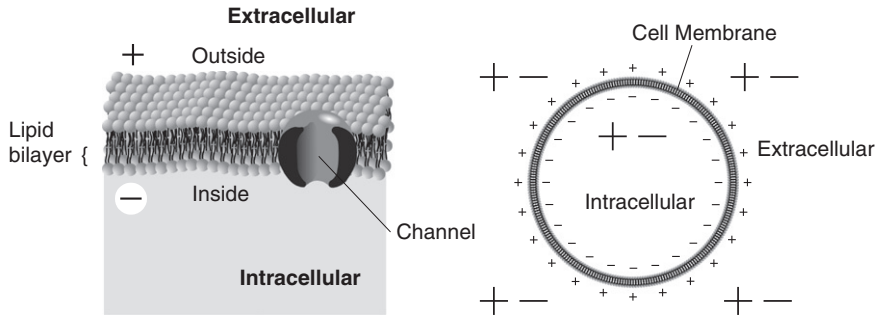

FIGURE 12.2 The separation of charges across a cell membrane. The figure on the left shows a cell membrane with positive ions along the outer surface of the cell membrane and negative ions along the inner surface of the cell membrane. The figure on the right further illustrates separation of charge by showing that only the ions along the inside and outside of the cell membrane are responsible for membrane potential (negative ions along the inside and positive ions along the outside of the cell membrane). Elsewhere the distribution of negative and positive ions are approximately evenly distributed as indicated with the large + − symbols for the illustration on the right. Overall, there is a net excess of negative ions inside the cell and a net excess of positive ions in the immediate vicinity outside the cell. For simplicity, the membrane shown on the right is drawn as the solid circle and ignores the axon and dendrites.

Graded Response and Action Potentials

A neuron can change the membrane potential of another neuron to which it is connected by releasing its neurotransmitter. The neurotransmitter crosses the synaptic cleft, interacts with receptor molecules in the postsynaptic membrane of the dendrite or cell body of the adjacent neuron, and changes the membrane potential of the receptor neuron (Figure 12.3).

The change in membrane potential at the postsynaptic membrane is due to a transformation from neurotransmitter chemical energy to electrical energy. The change in membrane potential depends on how much neurotransmitter is received and can be depolarizing or hyperpolarizing. This type of change in potential is typically called a *graded response*, since it varies with the amount of neurotransmitter received. Another way of envisaging the activity at the synapse is that the neurotransmitter received is integrated or summed, which results in a graded response in the membrane potential. Note that while a signal from a neuron is either inhibitory or excitatory, specific synapses may be excitatory and others inhibitory, providing the nervous system with the ability to perform complex tasks.

The net result of activation of the nerve cell is the action potential. The action potential is a large depolarizing signal of up to 100 mV that travels along the axon and lasts approximately 1–5 ms. Figure 12.4 illustrates a typical action potential. The action potential is an all or none signal that propagates actively along the axon without decreasing in amplitude. When the signal reaches the end of the axon at the presynaptic terminal, the change in potential causes the release of a packet of neurotransmitter. This is a very effective method of signaling over large distances. Additional details about the action potential are described throughout the remainder of this chapter after some tools for better understanding this phenomenon are introduced.

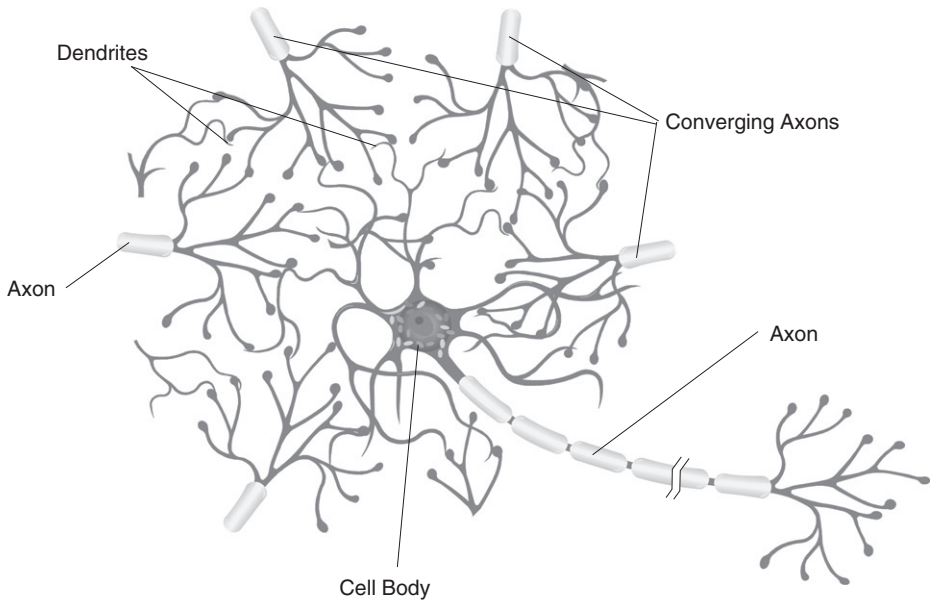

FIGURE 12.3 A typical neuron with presynaptic terminals of adjacent neurons in the vicinity of its dendrites.

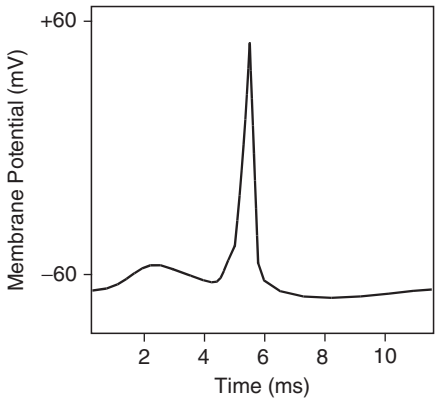

FIGURE 12.4 An action potential.

12.3.2 Resting Potential, Ionic Concentrations, and Channels

A resting membrane potential exists across the cell membrane because of the *differential distribution* of ions in and around the membrane of the nerve cell. The cell maintains these ion concentrations by using a selectively permeable membrane and, as described later, an active ion pump. A selectively permeable cell membrane with ion channels is illustrated in Figure 12.2. The neuron cell membrane is approximately 10 nm thick, and because it consists of a lipid bilayer (i.e., two plates separated by an insulator), it has capacitive properties. The extracellular fluid is composed of primarily Na^+ and Cl^-, and the intracellular fluid (cytosol) is composed of primarily K^+ and A^-. The large organic anions (A^-) are primarily amino acids and proteins that do not cross the membrane. Almost without exception, ions cannot pass through the cell membrane except through a channel.

Channels allow ions to pass through the membrane, are selective, and are either passive or active. Passive channels are always open and are ion specific. Figure 12.5 illustrates a cross section of a cell membrane with passive channels only. As shown, a particular channel allows only one ion type to pass through the membrane and prevents all other ions from crossing the membrane through that channel. Passive channels exist for Cl^-, K^+, and Na^+. In addition, a passive channel exists for Ca^{+2}, which is important in the excitation of the membrane at the synapse, as described in Section 12.8. Active channels, or gates, are either opened or closed in response to an external electrical or chemical stimulation. The active channels are also selective and allow only specific ions to pass through the membrane. Typically, active gates open in response to neurotransmitters and an appropriate change in membrane potential. Figure 12.6 illustrates the concept of an active channel. Here, K^+ passes through an active channel and Cl^- passes through a passive channel. As will be shown, passive channels are responsible for the resting membrane potential, and active channels are responsible for the graded response and action potentials.

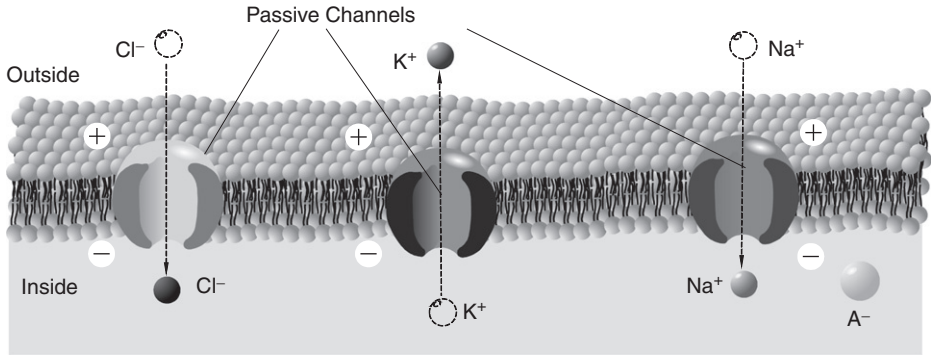

FIGURE 12.5 Idealized cross section of a selectively permeable membrane with channels for ions to cross the membrane. The thickness of the membrane and the size of the channels are not drawn to scale. When the diagram is drawn to scale, the cell membrane thickness is 20 times the size of the ions and 10 times the size of the channels, and the spacing between the channels is approximately 10 times the cell membrane thickness. Note that a potential difference exists between the inside and outside of the membrane, as illustrated with the + and – signs. The membrane is selectively permeable to ions through ion-specific channels—that is, each channel shown here only allows one particular ion to pass through it.

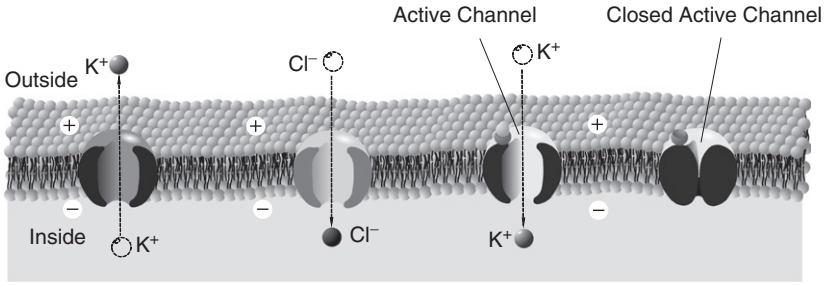

FIGURE 12.6 Passive and active channels provide a means for ions to pass through the membrane. Each channel is ion-specific. As shown, the active channel on the left allows K^+ to pass through the membrane, but the active channel on the right is not open, preventing any ion from passing through the membrane. Also shown is a passive Cl^- channel.

12.4 BASIC BIOPHYSICS TOOLS AND RELATIONSHIPS

12.4.1 Basic Laws

Two basic biophysics tools and a relationship are used to characterize the resting potential across a cell membrane by quantitatively describing the impact of the ionic gradient and electric field.

Fick's Law of Diffusion

The flow of particles due to diffusion is along the concentration gradient, with particles moving from high concentration areas to low ones. Specifically, for a cell membrane, the flow of ions across a membrane is given by

$$J(diffusion) = -D\frac{d[I]}{dx} \tag{12.1}$$

where J is the flow of ions due to diffusion, $[I]$ is the ion concentration, dx is the membrane thickness, and D is the diffusivity constant in m^2/s. The negative sign indicates that the flow of ions is from higher to lower concentration, and $\frac{d[I]}{dx}$ represents the concentration gradient. Fick's Law of diffusion was described in Section 7.3 involving a first-order differential equation that describes change in concentration as a function of time. Here, we are only interested in steady state.

Ohm's Law

Charged particles in a solution experience a force resulting from other charged particles and electric fields present. The flow of ions across a membrane is given by

$$J(drift) = -\mu Z[I]\frac{dv}{dx} \tag{12.2}$$

where J is the flow of ions due to drift in an electric field $\vec{E}$, μ = mobility in m^2/sV, Z = ionic valence, $[I]$ is the ion concentration, v is the voltage across the membrane, and $\frac{dv}{dx}$ is $(-\vec{E})$. Note that Z is positive for positively charged ions (e.g., Z = 1 for Na^+ and Z = 2 for Ca^{+2}) and negative for negatively charged ions (e.g., Z = −1 for Cl^-). Positive ions drift down the electric field and negative ions drift up the electric field.

Figure 12.7 illustrates a cell membrane that is permeable to only K^+ and shows the forces acting on K^+. Assume that the concentration of K^+ is that of a neuron with a higher concentration inside than outside and that the membrane resting potential is negative from inside to outside. Clearly, only K^+ can pass through the membrane, and Na^+, Cl^-, and A^- cannot move through it, since there are no channels for them to pass through. Depending on the actual concentration and membrane potential, K^+ will pass through the membrane until the forces due to drift and diffusion are balanced. The chemical force due to diffusion from inside to outside decreases as K^+ moves through the membrane, and the electric force increases as K^+ accumulates outside the cell until the two forces are balanced.

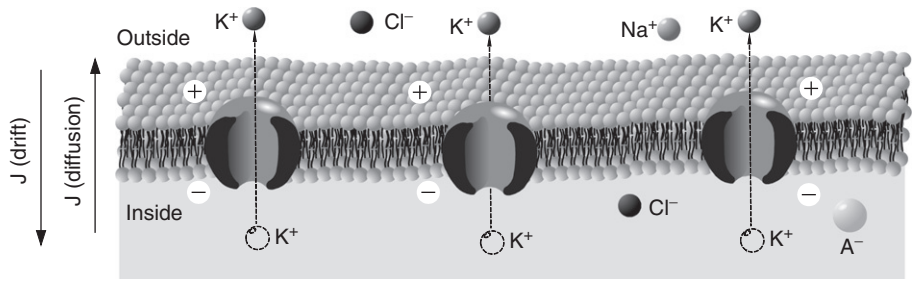

FIGURE 12.7 The direction of the flow of K^+ due to drift and diffusion across a cell membrane that is only permeable to K^+.

Einstein Relationship

The relationship between the drift of particles in an electric field under osmotic pressure described by Einstein in 1905 is given by

$$D = \frac{KT\mu}{q} \tag{12.3}$$

where D is the diffusivity constant, μ is mobility, K is Boltzmann's constant, T is the absolute temperature in degrees Kelvin, and q is the magnitude of the electric charge (i.e., 1.60186×10^{-19} coulombs).

12.4.2 Resting Potential of a Membrane Permeable to One Ion

The flow of ions in response to concentration gradients is limited by the selectively permeable nerve cell membrane and the resultant electric field. As described, ions pass through channels that are selective for that ion only. For clarity, the case of a membrane permeable to one ion only is considered first and then the case of a membrane permeable to more than one ion follows. It is interesting to note that neuroglial cells are permeable to only K^+ and that nerve cells are permeable to K^+, Na^+, and Cl^-. As will be shown, the normal ionic gradient is maintained if the membrane is permeable only to K^+ as in the neuroglial cell.

Consider the cell membrane shown in Figure 12.7 that is permeable only to K^+, and assume that the concentration of K^+ is higher in the intracellular fluid than the extracellular fluid. For this situation, the flow due to diffusion (concentration gradient) tends to push K^+ outside of the cell and is given by

$$J_K\,(diffusion) = -D\frac{d[K^+]}{dx} \tag{12.4}$$

The flow due to drift (electric field) tends to push K^+ inside the cell and is given by

$$J_K\,(drift) = -\mu Z[K^+]\frac{dv}{dx} \tag{12.5}$$

which results in a total flow

$$J_K = J_K\,(diffusion) + J_K\,(drift) = -D\frac{d[K^+]}{dx} - \mu Z[K^+]\frac{dv}{dx} \tag{12.6}$$

Using the Einstein relationship $D = \dfrac{KT\mu}{q}$, the total flow is now given by

$$J_K = -\frac{KT}{q}\mu\frac{d[K^+]}{dx} - \mu Z[K^+]\frac{dv}{dx} \tag{12.7}$$

From Eq. (12.7), the flow of K^+ is found at any time for any given set of initial conditions. In the special case of steady state—that is, at steady state when the flow of K^+ into the cell is exactly balanced by the flow out of the cell or $J_K = 0$—Eq. (12.7) reduces to

$$0 = -\frac{KT}{q}\mu\frac{d[K^+]}{dx} - \mu Z[K^+]\frac{dv}{dx} \tag{12.8}$$

With Z = +1, Eq. (12.8) simplifies to

$$dv = -\frac{KT}{q[K^+]}d[K^+] \tag{12.9}$$

Integrating Eq. (12.9) from outside the cell to inside yields

$$\int_{v_o}^{v_i} dv = -\frac{KT}{q}\int_{[K^+]_o}^{[K^+]_i}\frac{d[K^+]}{[K^+]} \tag{12.10}$$

where v_o and v_i are the voltages outside and inside the membrane, and $[K^+]_o$ and $[K^+]_i$ are the concentrations of potassium outside and inside the membrane. Thus,

$$v_i - v_o = -\frac{KT}{q}\ln\left(\frac{[K^+]_i}{[K^+]_o}\right) = \frac{KT}{q}\ln\left(\frac{[K^+]_o}{[K^+]_i}\right) \tag{12.11}$$

Equation (12.11) is known as the *Nernst equation*, named after German physical chemist Walter Nernst, and $E_K = v_i - v_o$ is known as the *Nernst potential* for K^+. At room temperature, $\frac{KT}{q} = 26\,mV$, and thus the Nernst equation for K^+ becomes

$$E_K = v_i - v_o = 26\ln\frac{[K^+]_o}{[K^+]_i}mV \tag{12.12}$$

While Eq. (12.12) is specifically written for K^+, it can be easily derived for any permeable ion. At room temperature, the Nernst potential for Na^+ is

$$E_{Na} = v_i - v_o = 26\ln\frac{[Na^+]_o}{[Na^+]_i}mV \tag{12.13}$$

and the Nernst potential for Cl^- is

$$E_{Cl} = v_i - v_o = -26\ln\frac{[Cl^-]_o}{[Cl^-]_i} = 26\ln\frac{[Cl^-]_i}{[Cl^-]_o}mV \tag{12.14}$$

The negative sign in Eq. (12.14) is due to Z = −1 for Cl^-.

12.4.3 Donnan Equilibrium

Consider a neuron at steady state that is permeable to more than one ion—for example, K^+, Na^+, and Cl^-. The Nernst potential for each ion can be calculated using Eqs. (12.12) to (12.14). The membrane potential, $V_m = v_i - v_o$, however, is due to the presence of all ions and is influenced by the concentration and permeability of each ion. In this section, the case in which two permeable ions are present is considered. In the next section, the case in which any number of permeable ions are present is considered.

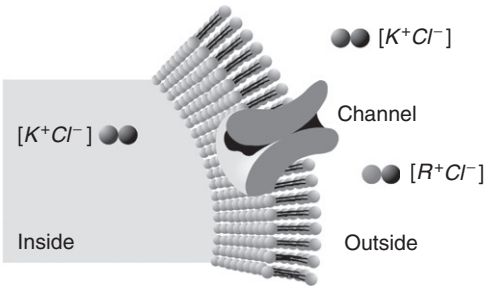

FIGURE 12.8 Membrane is permeable to both K^+ and Cl^-, but not to a large cation R^+.

Suppose a membrane is permeable to both K^+ and Cl^- but not to a large cation, R^+, as shown in Figure 12.8. Under steady-state conditions, the Nernst potentials for both K^+ and Cl^- must be equal—that is $E_K = E_{Cl}$, or

$$E_K = \frac{KT}{q} \ln \frac{[K^+]_o}{[K^+]_i} = E_{Cl} = \frac{KT}{q} \ln \frac{[Cl^-]_i}{[Cl^-]_o} \tag{12.15}$$

After simplifying,

$$\frac{[K^+]_o}{[K^+]_i} = \frac{[Cl^-]_i}{[Cl^-]_o} \tag{12.16}$$

Equation (12.16) is known as the *Donnan Equilibrium*. An accompanying principle is *space charge neutrality*, which states that the number of cations in a given volume is equal to the number of anions. Thus, at steady-state, ions still diffuse across the membrane, but each K^+ that crosses the membrane must be accompanied by a Cl^- for space charge neutrality to be satisfied. If in Figure 12.8 R^+ were not present, then at steady-state, the concentration of K^+ and Cl^- on both sides of the membrane would be equal. With R^+, the concentrations of [*KCl*] on both sides of the membrane are different, as shown in Example Problem 12.1, where R^+ is now in the intracellular fluid.

EXAMPLE PROBLEM 12.1

A membrane is permeable to K^+ and Cl^-, but not to a large cation R^+ as shown in the following figure. Find the steady-state concentration for the following initial conditions.

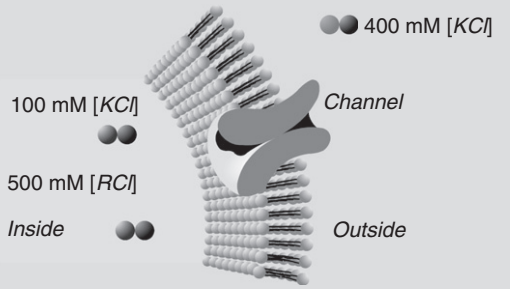

Continued

Solution

By conservation of mass,

$$[K^+]_i + [K^+]_o = 500$$

$$[Cl^-]_i + [Cl^-]_o = 1000$$

and space charge neutrality,

$$[K^+]_i + 500 = [Cl^-]_i$$

$$[K^+]_o = [Cl^-]_o$$

From the Donnan equilibrium,

$$\frac{[K^+]_o}{[K^+]_i} = \frac{[Cl^-]_i}{[Cl^-]_o}$$

Substituting for $[K^+]_o$ and $[Cl^-]_o$ from the conservation of mass equations into the Donnan equilibrium equation gives

$$\frac{500 - [K^+]_i}{[K^+]_i} = \frac{[Cl^-]_i}{1000 - [Cl^-]_i}$$

and eliminating $[Cl^-]_i$ by using the space charge neutrality equations gives

$$\frac{500 - [K^+]_i}{[K^+]_i} = \frac{[K^+]_i + 500}{1000 - [K^+]_i - 500} = \frac{[K^+]_i + 500}{500 - [K^+]_i}$$

Solving the preceding equation yields $[K^+]_i = 167$ mM at steady-state. Using the conservation of mass equations and space charge neutrality equation gives $[K^+]_o = 333$ mM, $[Cl^-]_i = 667$ mM, and $[Cl^-]_o = 333$ mM at steady-state. At steady-state and at room temperature, the Nernst potential for either ion is 18 mV, as shown for $[K^+]$:

$$E_K = v_i - v_o = 26 \ln \frac{333}{167} = 18\ mV$$

Summarizing, at steady-state

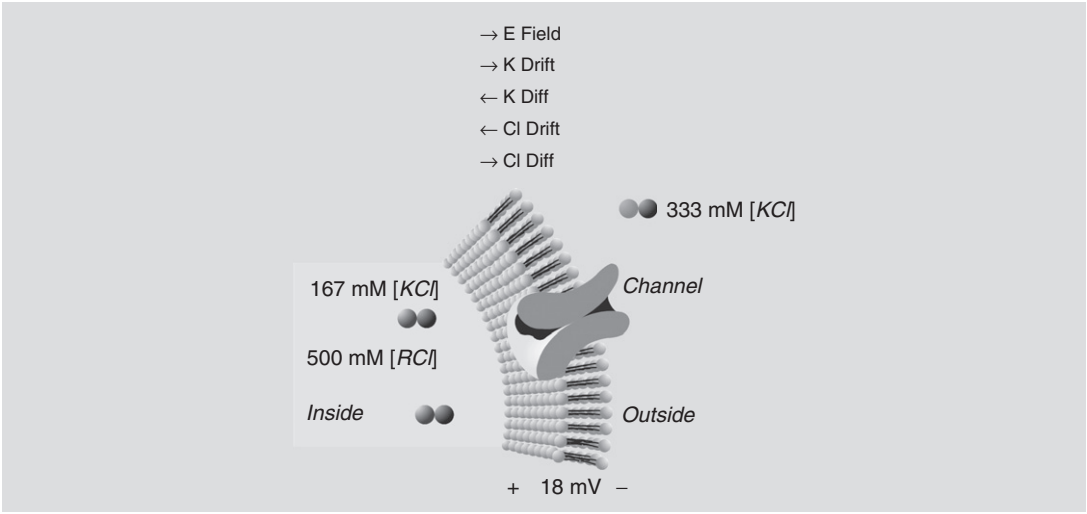

12.4.4 Goldman Equation

The squid giant axon resting potential is $-60\,mV$, which does not equal the Nernst potential for Na^+ or K^+. As a general rule, when V_m is affected by two or more ions, each ion influences V_m, as determined by its concentration and membrane permeability. The Goldman equation quantitatively describes the relationship between V_m and permeable ions, but only applies when the membrane potential or electric field is constant. This situation is a reasonable approximation for a resting membrane potential.

In this section, the Goldman equation is first derived for K^+ and Cl^-, and then extended to include K^+, Cl^-, and Na^+. The Goldman equation is used by physiologists to calculate the membrane potential for a variety of cells and, in fact, was used by Hodgkin, Huxley, and Katz in studying the squid giant axon.

Consider the cell membrane shown in Figure 12.9. To determine V_m for both K^+ and Cl^-, flow equations for each ion are derived separately under the condition of a constant electric

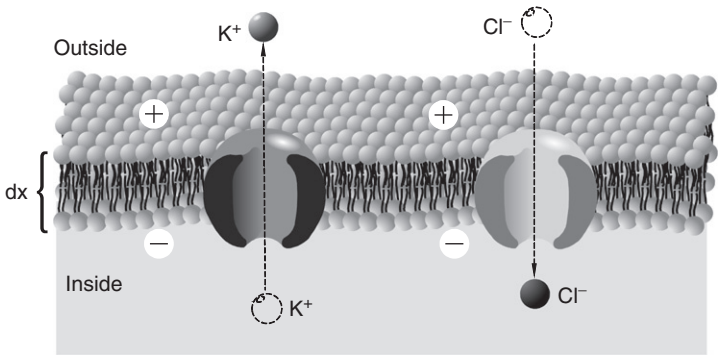

FIGURE 12.9 A cell membrane that is permeable to both K^+ and Cl^-. The width of the membrane is $dx = \delta$.

field and then combined using space charge neutrality to complete the derivation of the Goldman equation.

Potassium Ions

The flow equation for K^+ with mobility μ_K is

$$J_K = -\frac{KT}{q}\mu_K \frac{d[K^+]}{dx} - \mu_K Z_K [K^+]\frac{dv}{dx} \tag{12.17}$$

Under a constant electric field,

$$\frac{dv}{dx} = \frac{\Delta v}{\Delta x} = \frac{V}{\delta} \tag{12.18}$$

Substituting Eq. (12.18) into (12.17) with $Z_K = 1$ gives

$$J_K = -\frac{KT}{q}\mu_K \frac{d[K^+]}{dx} - \mu_K [K^+]\frac{V}{\delta} \tag{12.19}$$

Let the permeability for K^+, P_K, equal

$$P_K = \frac{\mu_K KT}{\delta q} = \frac{D_K}{\delta} \tag{12.20}$$

Substituting Eq. (12.20) into (12.19) gives

$$J_K = \frac{-P_K q}{KT} V[K^+] - P_K \delta \frac{d[K^+]}{dx} \tag{12.21}$$

Rearranging the terms in Eq. (12.21) yields

$$dx = \frac{d[K^+]}{\frac{-J_K}{P_K \delta} - \frac{qV[K^+]}{KT\delta}} \tag{12.22}$$

Taking the integral of both sides, while assuming that J_K is independent of x, gives

$$\int_0^{\delta} dx = \int_{[K^+]_i}^{[K^+]_o} \frac{d[K^+]}{\frac{-J_K}{P_K \delta} - \frac{qV[K^+]}{KT\delta}} \tag{12.23}$$

resulting in

$$x\Big|_0^{\delta} = -\frac{KT\delta}{qV} \ln\left(\frac{J_K}{P_K \delta} + \frac{qV[K^+]}{KT\delta}\right)\Bigg|_{[K^+]_i}^{[K^+]_o} \tag{12.24}$$

and

$$\delta = -\frac{KT\delta}{qV} \ln\left(\frac{\frac{J_K}{P_K \delta} + \frac{qV[K^+]_o}{KT\delta}}{\frac{J_K}{P_K \delta} + \frac{qV[K^+]_i}{KT\delta}}\right) \tag{12.25}$$

Removing δ from both sides of Eq. (12.25), bringing the term $-\frac{KT}{qV}$ to the other side of the equation, and then taking the exponential of both sides yields

$$e^{-\frac{qV}{KT}} = \frac{\frac{J_K}{P_K\delta} + \frac{qV[K^+]_o}{KT\delta}}{\frac{J_K}{P_K\delta} + \frac{qV[K^+]_i}{KT\delta}} \tag{12.26}$$

Solving for J_K in Eq. (12.26) gives

$$J_K = \frac{qVP_K}{KT}\left(\frac{[K^+]_o - [K^+]_i e^{\frac{-qV}{KT}}}{e^{\frac{-qV}{KT}} - 1}\right) \tag{12.27}$$

Chlorine Ions

The same derivation carried out for K^+ can be repeated for Cl^-, which yields

$$J_{Cl} = \frac{qVP_{Cl}}{KT}\left(\frac{[Cl^-]_o e^{\frac{-qV}{KT}} - [Cl^-]_i}{e^{\frac{-qV}{KT}} - 1}\right) \tag{12.28}$$

where P_{Cl} is the permeability for Cl^-.

Summarizing for Potassium and Chlorine Ions

Using space charge neutrality, $J_K = J_{Cl}$, and Eqs. (12.27) and (12.28) gives

$$P_K\left([K^+]_o - [K^+]_i e^{\frac{-qV}{KT}}\right) = P_{Cl}\left([Cl^-]_o e^{\frac{-qV}{KT}} - [Cl^-]_i\right) \tag{12.29}$$

Solving for the exponential terms yields

$$e^{\frac{-qV}{KT}} = \frac{P_K[K^+]_o + P_{Cl}[Cl^-]_i}{P_K[K^+]_i + P_{Cl}[Cl^-]_o} \tag{12.30}$$

Solving for V gives

$$V = v_o - v_i = -\frac{KT}{q}\ln\left(\frac{P_K[K^+]_o + P_{Cl}[Cl^-]_i}{P_K[K^+]_i + P_{Cl}[Cl^-]_o}\right) \tag{12.31}$$

or in terms of V_m

$$V_m = \frac{KT}{q}\ln\left(\frac{P_K[K^+]_o + P_{Cl}[Cl^-]_i}{P_K[K^+]_i + P_{Cl}[Cl^-]_o}\right) \tag{12.32}$$

This equation is called the *Goldman equation*. Since sodium is also important in membrane potential, the Goldman equation for K^+, Cl^-, and Na^+ can be derived as

$$V_m = \frac{KT}{q}\ln\left(\frac{P_K[K^+]_o + P_{Na}[Na^+]_o + P_{Cl}[Cl^-]_i}{P_K[K^+]_i + P_{Na}[Na^+]_i + P_{Cl}[Cl^-]_o}\right) \tag{12.33}$$

where P_{Na} is the permeability for Na^+. To derive Eq. (12.33), first find J_{Na} and then use space charge neutrality $J_K + J_{Na} = J_{Cl}$. Equation (12.33) then follows. In general, when the

TABLE 12.1 Approximate Intracellular and Extracellular Concentrations of the Important Ions across a Squid Giant Axon, Ratio of Permeabilities, and Nernst Potentials

Ion	Cytoplasm (mM)	Extracellular Fluid (mM)	Ratio of Permeabilities	Nernst Potential (mV)
K^+	400	20	1	−74
Na^+	50	440	0.04	55
Cl^-	52	560	0.45	−60

Note: Permeabilities are relative—that is, P_K:P_{Na}:P_{Cl}—and not absolute. Data were recorded at 6.3°C, resulting in KT/q approximately equal to 25.3 mV.

TABLE 12.2 Approximate Intracellular and Extracellular Concentrations of the Important Ions across a Frog Skeletal Muscle, Ratio of Permeabilities, and Nernst Potentials

Ion	Cytoplasm (mM)	Extracellular Fluid (mM)	Ratio of Permeabilities	Nernst Potential (mV)
K^+	140	2.5	1.0	–105
Na^+	13	110	0.019	56
Cl^-	3	90	0.381	–89

Note: Data were recorded at room temperature, resulting in KT/q approximately equal to 26 mV.

permeability to one ion is exceptionally high, as compared with the other ions, then V_m predicted by the Goldman equation is very close to the Nernst equation for that ion.

Tables 12.1 and 12.2 contain the important ions across the cell membrane, the ratio of permeabilities, and Nernst potentials for the squid giant axon and frog skeletal muscle. The squid giant axon is extensively reported and used in experiments due to its large size, lack of myelination, and ease of use. In general, the intracellular and extracellular concentration of ions in vertebrate neurons is approximately three to four times less than the squid giant axon.

EXAMPLE PROBLEM 12.2

Calculate V_m for the squid giant axon at 6.3°C.

Solution

Using Equation (12.33) and the data in Table 12.1 gives

$$V_m = 25.3 \times \ln\left(\frac{1 \times 20 + 0.04 \times 440 + 0.45 \times 52}{1 \times 400 + 0.04 \times 50 + 0.45 \times 560}\right) mV = -60\, mV$$

12.4.5 Ion Pumps

At rest, separation of charge and ionic concentrations across the cell membrane must be maintained, or V_m changes. That is, the flow of charge into the cell must be balanced by the flow of charge out of the cell. For Na^+, the concentration and electric gradient creates a force

that drives Na^+ into the cell at rest. At V_m, the K^+ force due to diffusion is greater than that due to drift and results in an efflux of K^+ out of the cell. Space charge neutrality requires that the influx of Na^+ be equal to the flow of K^+ out of the cell. Although these flows cancel out each other and space charge neutrality is maintained, this process cannot continue unopposed. Otherwise, $[K^+]_i$ goes to zero as $[Na^+]_i$ increases, with subsequent change in V_m as predicted by the Goldman equation.

Any change in the concentration gradient of K^+ and Na^+ is prevented by the *Na-K* pump. The pump transports a steady stream of Na^+ out of the cell and K^+ into the cell. Removal of Na^+ from the cell is against its concentration and electric gradient and is accomplished with an active pump that consumes metabolic energy. The biochemical reactions that govern the *Na-K* pump are given in Chapter 8. The *Na-K* pump is also used to maintain cell volume. Figure 12.10 illustrates an *Na-K* pump along with passive channels.

The *Na-K* pump has been found to be electrogenic—that is, there is a net transfer of charge across the membrane. Nonelectrogenic pumps operate without any net transfer of charge. For many neurons, the *Na-K* ion pump removes three Na^+ ions for every two K^+ ions moved into the cell, which makes V_m slightly more negative than predicted with only passive channels.

In general, when the cell membrane is at rest, the active and passive ion flows are balanced and a permanent potential exists across a membrane only under the following conditions:

1. The membrane is impermeable to some ion(s).
2. An active pump is present.

The presence of the *Na-K* pump forces V_m to a given potential based on the $K^+$and Na^+ concentrations that are determined by the active pump. Other ion concentrations are determined by V_m. For instance, since Cl^- moves across the membrane only through passive channels, the Cl^- concentration ratio at rest is determined from the Nernst equation with $E_{Cl} = V_m$, or

$$\frac{[Cl^-]_i}{[Cl^-]_o} = e^{\frac{qV_m}{KT}} \tag{12.34}$$

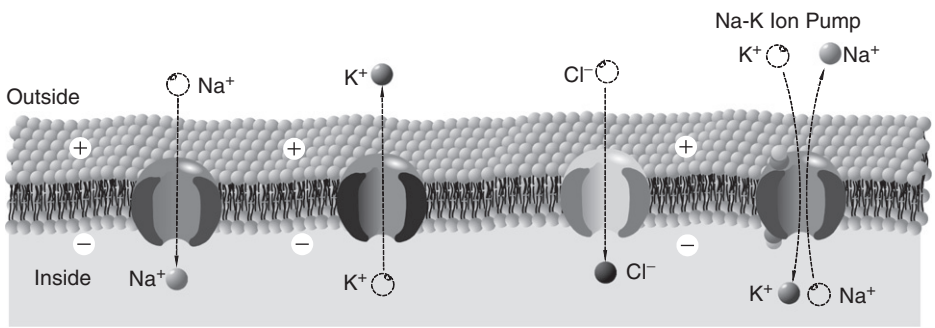

FIGURE 12.10 An active pump is illustrated along with passive channels.

EXAMPLE PROBLEM 12.3

Consider a membrane in which there is an active K^+ pump, passive channels for K^+ and Cl^-, and a non-steady-state initial concentration of $[KCl]$ on both sides of the membrane. Find an expression for the active K^+ pump.

Solution

From space charge neutrality, $J_{Cl} = J_K$, or

$$J_K = J_p - \mu_K Z_K [K^+] \frac{dv}{dx} - \frac{KT}{q} \mu_K \frac{d[K^+]}{dx}$$

$$J_{Cl} = -\mu_{Cl} Z_{Cl} [Cl^-] \frac{dv}{dx} - \frac{KT}{q} \mu_{Cl} \frac{d[Cl^-]}{dx}$$

where J_p is the flow due to the active K^+ pump. Solving for $\frac{dv}{dx}$ using the J_{Cl} equation with $Z_{Cl} = -1$ gives

$$\frac{dv}{dx} = \frac{KT}{q[Cl^-]} \frac{d[Cl^-]}{dx}$$

By space charge neutrality, $[Cl^-] = [K^+]$, which allows rewriting the previous equation as

$$\frac{dv}{dx} = \frac{KT}{q[K^+]} \frac{d[K^+]}{dx}$$

At steady state, both flows are zero, and with $Z_K = 1$, the J_K equation with $\frac{dv}{dx}$ substitution is given as

$$\begin{aligned} J_K = 0 &= J_p - \mu_K [K^+] \frac{dv}{dx} - \frac{KT\mu_K}{q} \frac{d[K^+]}{dx} \\ &= J_p - \mu_K [K^+] \frac{KT}{q[K^+]} \frac{d[K^+]}{dx} - \frac{KT\mu_K}{q} \frac{d[K^+]}{dx} \\ &= J_p - \frac{2KT\mu_K}{q} \frac{d[K^+]}{dx} \end{aligned}$$

Moving J_p to the left side of the equation, multiplying both sides by dx, and then integrating yields

$$-\int_0^{\delta} J_p dx = -\frac{2KT\mu_K}{q} \int_{[K^+]_i}^{[K^+]_o} d[K^+]$$

or

$$J_p = \frac{2KT\mu_K}{q\delta} \left([K^+]_o - [K^+]_i \right)$$

Note: If *no* pump was present in this example, then at steady-state, the concentration on both sides of the membrane would be the same.

12.5 EQUIVALENT CIRCUIT MODEL FOR THE CELL MEMBRANE

In this section, an equivalent circuit model is developed using the tools previously developed. Creating a circuit model is helpful when discussing the Hodgkin-Huxley model of an action potential in the next section, a model that introduces voltage- and time-dependent ion channels. As previously described, the nerve has three types of passive electrical characteristics: electromotive force, resistance, and capacitance. The nerve membrane is a lipid bilayer that is pierced by a variety of different types of ion channels, where each channel is characterized as being passive (always open) or active (gates that can be opened). Each ion channel is also characterized by its selectivity. In addition, there is the active *Na-K* pump that maintains V_m across the cell membrane at steady state.

12.5.1 Electromotive, Resistive, and Capacitive Properties

Electromotive Force Properties

The three major ions, K^+, Na^+, and Cl^-, are differentially distributed across the cell membrane at rest using passive ion channels, as illustrated in Figure 12.5. This separation of charge exists across the membrane and results in a voltage potential V_m, as described by Eq. (12.33) (the Goldman equation).

Across each ion-specific channel, a concentration gradient exists for each ion that creates an electromotive force, a force that drives that ion through the channel at a constant rate. The Nernst potential for that ion is the electrical potential difference across the channel and is easily modeled as a battery, as shown in Figure 12.11 for K^+. The same model is applied for Na^+ and Cl^-, with values equal to the Nernst potentials for each.

Resistive Properties

In addition to the electromotive force, each channel also has resistance—that is, it resists the movement of ions through the channel. This is mainly due to collisions with the channel wall, where energy is given up as heat. The term conductance, G, measured in siemens (S), which is the ease with which the ions move through the membrane, is typically used to

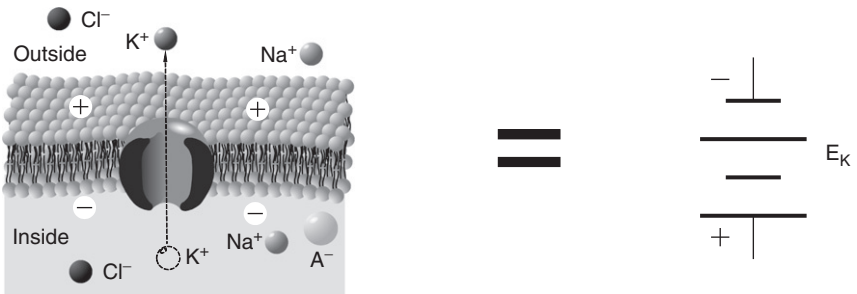

FIGURE 12.11 A battery is used to model the electromotive force for a K^+ channel with a value equal to the K^+ Nernst potential. The polarity of the battery is given with the ground on the outside of the membrane in agreement with convention. From Table 12.1, note that the Nernst potential for K^+ is negative, which reverses the polarity of the battery, driving K^+ out of the cell.

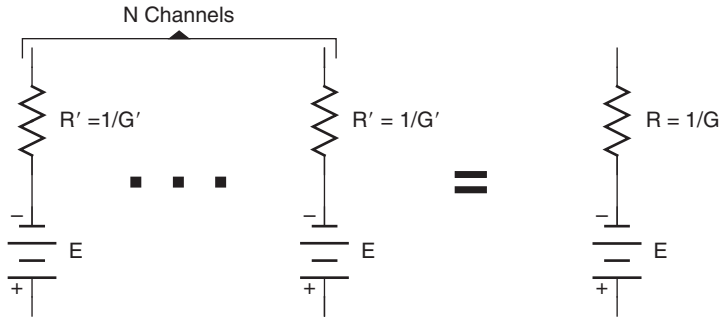

FIGURE 12.12 The equivalent circuit for N ion channels is a single resistor and battery.

represent resistance. Since the conductances (channels) are in parallel, the total conductance is the total number of channels, N, times the conductance for each channel, G':

$$G = N \times G'$$

It is usually more convenient to write the conductance as resistance $R = \frac{1}{G}$, measured in ohms (Ω). An equivalent circuit for the channels for a single ion is now given as a resistor in series with a battery, as shown in Figure 12.12.

Conductance is related to membrane permeability, but they are not interchangeable in a physiological sense. Conductance depends on the state of the membrane, varies with ion concentration, and is proportional to the flow of ions through a membrane. Permeability describes the state of the membrane for a particular ion. Consider the case in which there are no ions on either side of the membrane. No matter how many channels are open, G = 0 because there are no ions available to flow across the cell membrane (due to a potential difference). At the same time, ion permeability is constant and determined by the state of the membrane.

Equivalent Circuit for Three Ions

Each of the three ions $K^+, Na^+,$ and Cl^- are represented by the same equivalent circuit, as shown in Figure 12.12, with Nernst potentials and appropriate resistances. Combining the three equivalent circuits into one circuit with the extracellular fluid and cytoplasm connected by short circuits completely describes a membrane at rest (Figure 12.13).

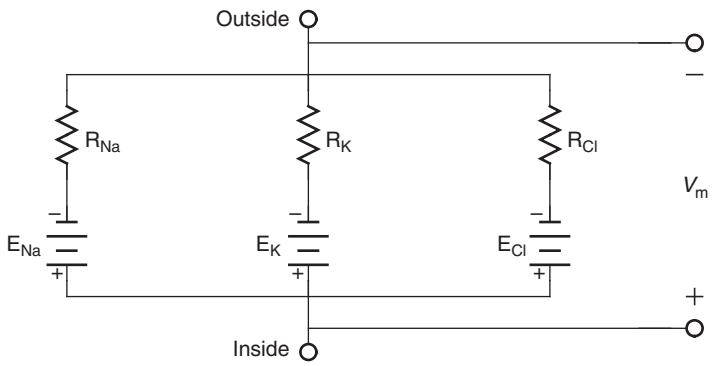

FIGURE 12.13 Model of the passive channels for a small area of nerve at rest, with each ion channel represented by a resistor in series with a battery.

EXAMPLE PROBLEM 12.4

Find V_m for the frog skeletal muscle (Table 12.2) if the Cl^- channels are ignored. Use $R_K = 1.7\ \text{k}\Omega$ and $R_{Na} = 15.67\ \text{k}\Omega$.

Solution

The following diagram depicts the membrane circuit with mesh current I, current I_{Na} through the sodium channel, and current I_K through the potassium channel. Current I is found using mesh analysis:

$$E_{Na} + IR_{Na} + IR_K - E_K = 0$$

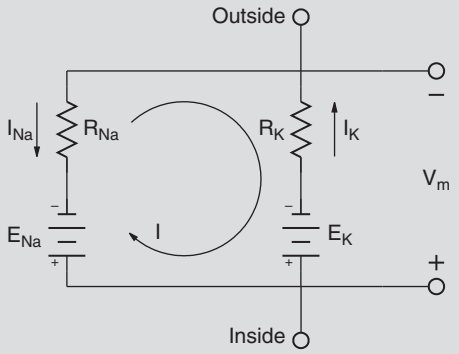

and then solving for I,

$$I = \frac{E_K - E_{Na}}{R_{Na} + R_K} = \frac{(-105 - 56) \times 10^{-3}}{(15.67 + 1.7) \times 10^3} = -9.27\ \mu A$$

yields

$$V_m = E_{Na} + IR_{Na} = -89\ mV$$

Notice that $I = -I_{Na}$ and $I = -I_K$, or $I_{Na} = I_K$ as expected. Physiologically, this implies that the inward Na^+ current is exactly balanced by the outward bound K^+ current.

EXAMPLE PROBLEM 12.5

Find Vm for the frog skeletal muscle if $R_{Cl} = 3.125\ \text{k}\Omega$.

Solution

To solve, first find a Thevenin's equivalent circuit for the circuit in Example Problem 12.4:

$$V_{TH} = V_m = -89\ \text{mV}$$

and

$$R_{TH} = \frac{R_{Na} \times R_K}{R_{Na} + R_K} = 1.534\ \text{k}\Omega$$

Continued

The Thevenin's equivalent circuit is shown in the following figure.

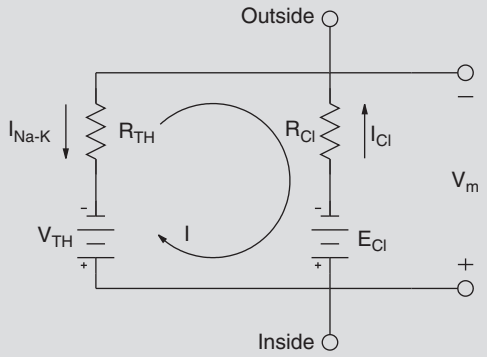

Since $E_{Cl} = V_{TH}$ according to Table 12.2, no current flows. This is the actual situation in most nerve cells. The membrane potential is determined by the relative conductances and Nernst potentials for K^+ and Na^+. The Nernst potentials are maintained by the *Na-K* active pump that maintains the concentration gradient. Cl^- is usually passively distributed across the membrane.

The Na-K *Pump*

As shown in Example Problem 12.4 and Section 12.4, there is a steady flow of K^+ ions out of the cell and Na^+ ions into the cell even when the membrane is at the resting potential. Left unchecked, this would drive E_K and E_{Na} toward 0. To prevent this, current generators depicting the *Na-K* pump are used that are equal to and the opposite of the passive currents and incorporated into the model, as shown in Figure 12.14.

12.5.2 Capacitive Properties

Capacitance occurs whenever electrical conductors are separated by an insulating material. In the neuron, the cytoplasm and extracellular fluid are the electrical conductors,

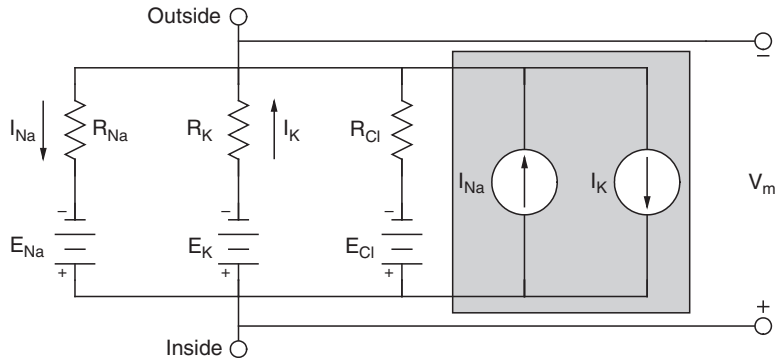

FIGURE 12.14 Circuit model of the three passive channels for a small area of the nerve at rest with each ion channel represented by a resistor in series with a battery. The *Na-K* active pump is modeled as two current sources within the shaded box.

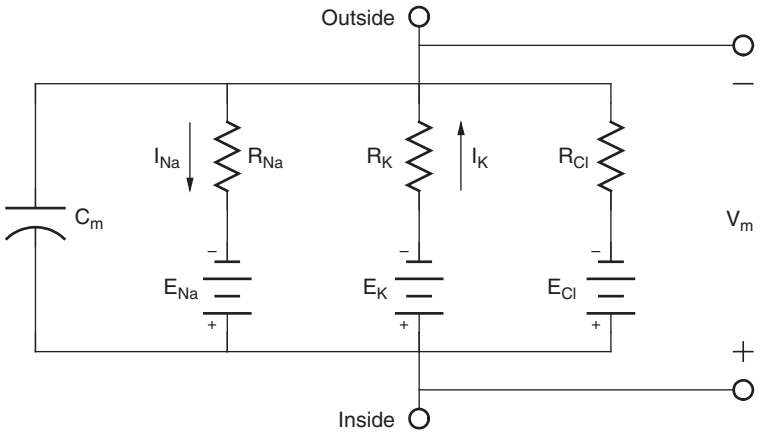

FIGURE 12.15 Circuit model of a small area of the nerve at rest with all of its passive electrical properties. The *Na-K* active pump shown in Figure 12.14 is removed, since it does not contribute electrically to the circuit.

and the lipid bilayer of the membrane is the insulating material (see Figure 12.3). Capacitance for a neuron membrane is approximately $1\mu F/cm^2$. Membrane capacitance implies that ions do not move through the membrane except through ion channels.

The membrane can be modeled using the circuit in Figure 12.15 by incorporating membrane capacitance with the electromotive and resistive properties. A consequence of membrane capacitance is that changes in membrane voltage are not immediate but follow an exponential time course due to first-order time constant effects. To appreciate the effect of capacitance, the circuit in Figure 12.15 is reduced to Figure 12.16 by using a Thevenin's equivalent for the batteries and the resistors with R_{TH} and V_{TH} given in Eqs. (12.35) and (12.36).

$$R_{TH} = \frac{1}{\frac{1}{R_K} + \frac{1}{R_{Na}} + \frac{1}{R_{Cl}}} \tag{12.35}$$

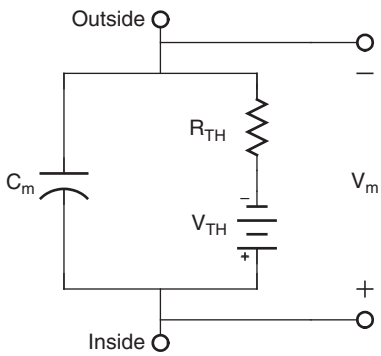

FIGURE 12.16 Thévenin's equivalent circuit of the model in Figure 12.15.

$$V_{TH} = \frac{R_{Na}R_{Cl}E_K + R_K R_{Cl}E_{Na} + R_K R_{Na}E_{Cl}}{R_{Na}R_{Cl} + R_K R_{Cl} + R_K R_{Na}} \tag{12.36}$$

The time constant for the membrane circuit model is $\tau = R_{TH}C_m$, and at 5τ the response is within 1 percent of steady-state. The range for τ is from 1 to 20 ms in a typical neuron. In addition, at steady-state the capacitor acts as an open circuit and $V_{TH} = V_m$, as it should.

EXAMPLE PROBLEM 12.6

Compute the change in V_m due to a current pulse through the cell membrane.

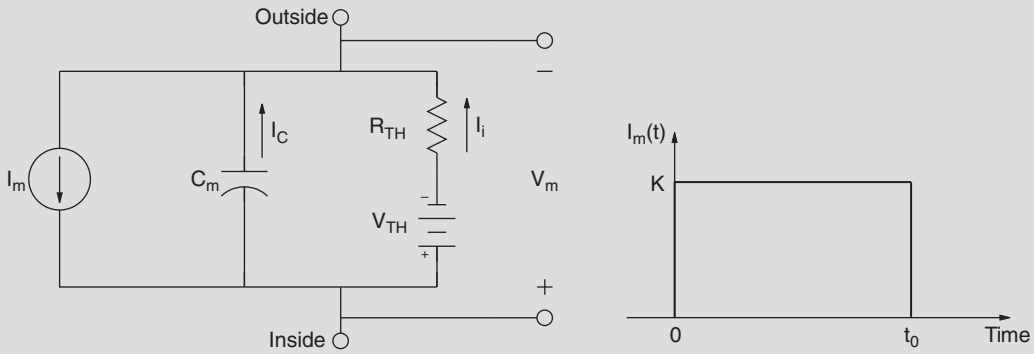

Solution

Experimentally, the stimulus current is a pulse passed through the membrane from an intracellular electrode to an extracellular electrode, as depicted in the circuit diagram above. The membrane potential, V_m, due to a current pulse, I_m, with amplitude K and duration t_0 applied at $t = 0$, is found by applying Kirchhoff's current law at the cytoplasm, yielding

$$-I_m + \frac{V_m - V_{TH}}{R_{TH}} + C_m \frac{dV_m}{dt} = 0$$

The Laplace transform of the node equation is

$$-I_m(s) + \frac{V_m(s)}{R_{TH}} - \frac{V_{TH}}{sR_{TH}} + sC_m V_m(s) - C_m V_m(0^+) = 0$$

Combining common terms gives

$$\left(s + \frac{1}{C_m R_{TH}}\right) V_m(s) = V_m(0^+) + \frac{I_m(s)}{C_m} + \frac{V_{TH}}{sC_m R_{TH}}$$

The Laplace transform of the current pulse is $I_m(s) = \frac{K}{s}\left(1 - e^{-st_0}\right)$. Substituting $I_m(s)$ into the node equation and rearranging terms yields

$$V_m(s) = \frac{V_m(0^+)}{\left(s + \frac{1}{C_m R_{TH}}\right)} + \frac{K(1 - e^{st_0})}{sC_m\left(s + \frac{1}{C_m R_{TH}}\right)} + \frac{V_m}{sC_m R_{TH}\left(s + \frac{1}{C_m R_{TH}}\right)}$$

Performing a partial fraction expansion, and noting that $V_m(0^+) = V_{TH}$, gives

$$V_m(s) = KR_{TH}\left(\frac{1}{s} - \frac{1}{\left(s + \frac{1}{C_m R_{TH}}\right)}\right)\left(1 - e^{-st_0}\right) + \frac{V_{TH}}{s}$$

Transforming back into the time domain yields the solution

$$V_m(t) = V_{TH} + R_{TH}K\left(1 - e^{-\frac{t}{R_{TH}C_m}}\right)u(t) - R_{TH}K\left(1 - e^{-\frac{t-t_0}{R_{TH}C_m}}\right)u(t - t_0)$$

The ionic current (I_i) and capacitive current (I_c) are shown in the following figure, where

$$I_i = \frac{V_m - V_{TH}}{R_{Th}}$$

$$I_c = C_m \frac{dV_m}{dt}$$

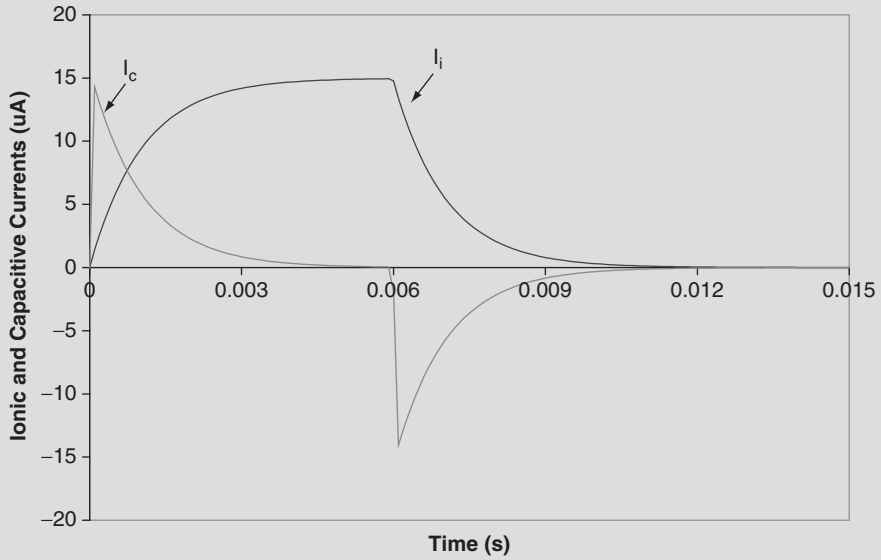

Shown in the following figures are graphs of V_m in response to a 15 μA current pulse of 6 ms (top) and 2 ms (bottom) using parameters for the frog skeletal muscle. The time constant is

Continued

approximately 1 ms. Note that in the figure on the top, V_m reaches steady state before the current pulse returns to zero, and in the figure on the bottom, V_m falls short of the steady state value reached on the top. The value of the time constant is important in the integration of currents (packets of neurotransmitter) at the synapse. Each packet of neurotransmitter acts as a current pulse, as described in Section 12.8. Note that the longer the time constant, the more time the membrane is excited. Most excitations are not synchronous, but because of τ, a significant portion of the stimulus is added together that might cause an action potential.

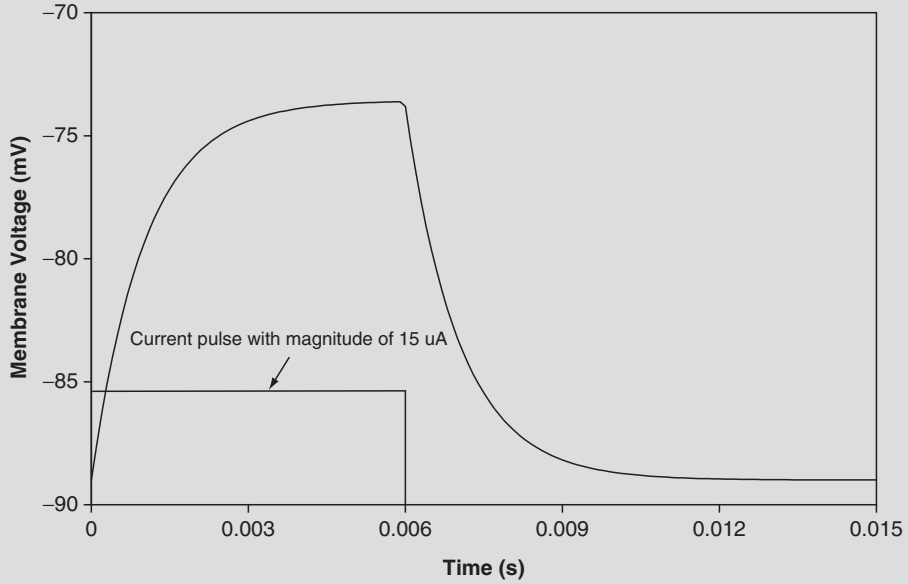

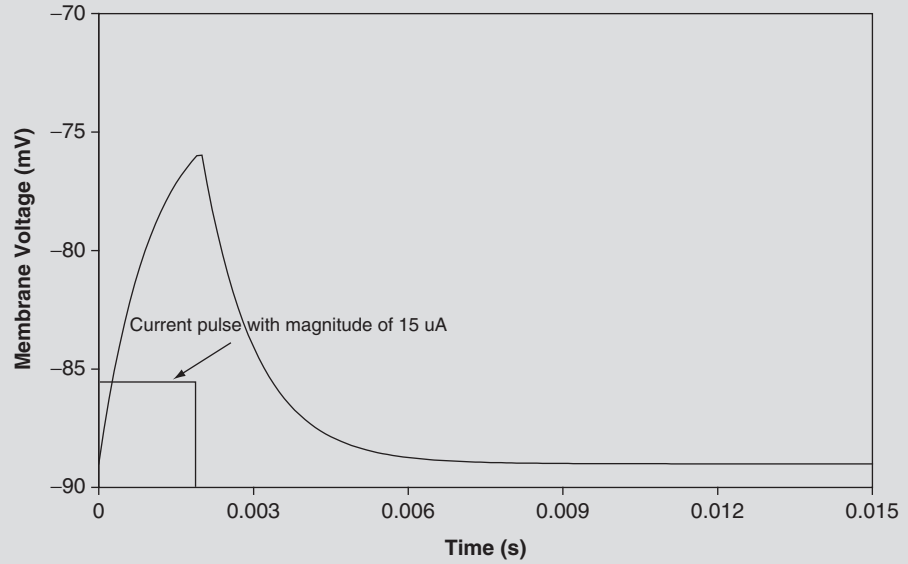

The following figure is due to a series of 15 μA current pulses of 6 ms duration, with the onsets occurring at 0, 2, 4, 6, and 8 ms. Since the pulses occur within 5τ of the previous pulses, the effect of each on V_m is additive, allowing the membrane to depolarize to approximately −45 mV. If the pulses are spaced at intervals greater than 5τ, then V_m would be a series of pulse responses, as previously illustrated.

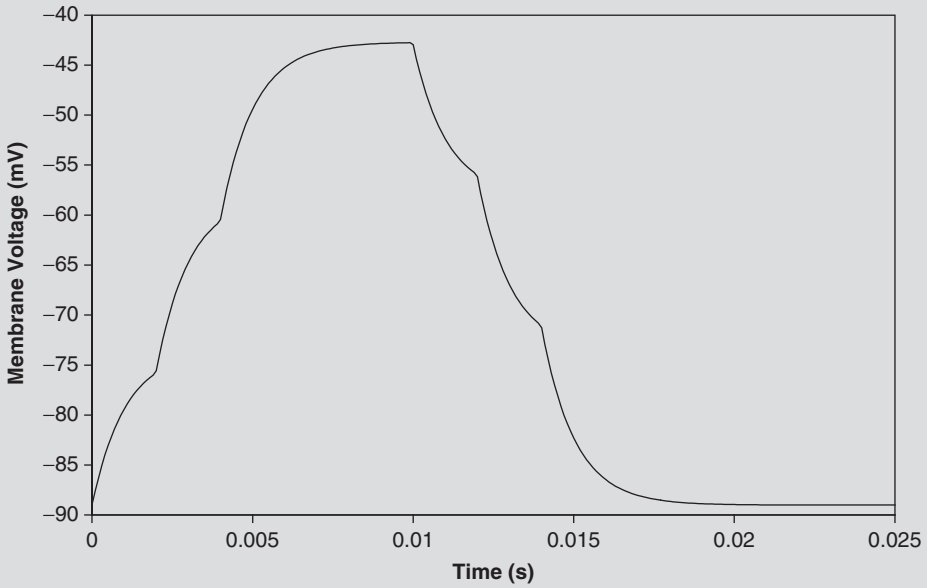

12.5.3 Changes in Membrane Potential with Distance

The circuit model in Figure 12.15 or 12.16 describes a small area or section of the membrane. In Example Problem 12.6, a current pulse was injected into the membrane and resulted in a change in V_m. The change in V_m in this section of the membrane causes current to flow into the adjacent membrane sections, which causes a change in V_m in each section and so on, continuing throughout the surface of the membrane. Since the volume inside the dendrite is much smaller than the extracellular space, there is significant resistance to the flow of current in the cytoplasm from one membrane section to the next as compared with the flow of current in the extracellular space. The larger the diameter of the dendrite, the smaller the resistance to the spread of current from one section to the next. To model this effect, a resistor, R_a, is placed in the cytoplasm connecting each section together, as shown in Figure 12.17. This model is actually a three-dimensional surface and continues in the x, y, and z directions. The outside resistance is negligible, since it has a greater volume and is modeled as a short circuit.

Suppose a current is injected into a section of the dendrite as shown in Figure 12.18, similar to the situation in Example Problem 12.6, where t_0 is large. At steady state, the transient response due to C_m has expired, and only current through the resistance is important. Most of the current flows out through the section into which the current was injected, since it has

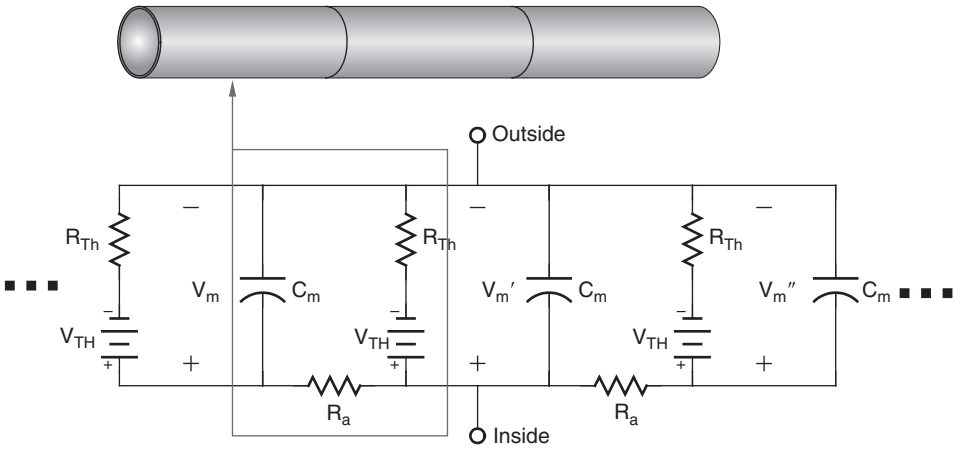

FIGURE 12.17 Equivalent circuit of series of membrane sections connected with axial resistance, R_a.

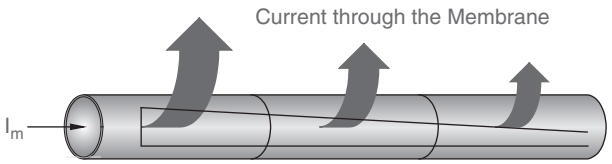

FIGURE 12.18 The flow of current through a dendrite at steady-state. Since current seeks the path of least resistance, most of the current leaves the dendrite at the injection site and becomes smaller with distance from the injection site.

the smallest resistance (R_{TH}) in relation to the other sections. The next largest current flowing out of the membrane occurs in the next section, since it has the next smallest resistance, $R_{TH} + R_a$. The change in V_m, ΔV_m, from the injection site is independent of C_m and depends solely on the relative values of R_{TH} and R_a. The resistance seen n sections from the injection site is $R_{TH} + nR_a$. Since current decreases with distance from the injection site, then ΔV_m also decreases with distance from the injection site because it equals the current through that section times R_{TH}. The change in membrane potential, ΔV_m, decreases exponentially with distance and is given by

$$\Delta V_m = V_o e^{\frac{-x}{\lambda}} \tag{12.37}$$

where $\lambda = \sqrt{\frac{R_{TH}}{R_a}}$ is the membrane length constant, x is the distance away from injection site, and V_o is the change in membrane potential at the injection site.[1] The range of values for λ is 0.1 to 1 mm. The larger the value of λ, the greater the effect of the stimulation along the length of the membrane.

[1]Equation 12.37 is the solution of the one dimensional cable equation for the dendrite using partial differential equations (see Keener and Sneyd for details).

12.6 THE HODGKIN-HUXLEY MODEL OF THE ACTION POTENTIAL

Alan Lloyd Hodgkin and Andrew Fielding Huxley published five papers in 1952 that described a series of experiments and an empirical model of an action potential in a squid giant axon. Their first four papers described the experiments that characterized the changes in the cell membrane that occurred during the action potential. The last paper presented the empirical model. The empirical model they developed is not a physiological model based on the laws and theory developed in this chapter but a model based on curve fitting using an exponential function. In this section, highlights of the Hodgkin-Huxley experiments are presented along with the empirical model. All of the figures presented in this section were simulated using SIMULINK and the Hodgkin-Huxley empirical model parameterized with their squid giant axon data.

12.6.1 Action Potentials and the Voltage Clamp Experiment

The ability of nerve cells to conduct action potentials makes it possible for signals to be transmitted over long distances within the nervous system. An important feature of the action potential is that it does not decrease in amplitude as it is conducted away from its site of initiation. An action potential occurs when V_m reaches a value called the *threshold potential* at the axon hillock (see Figure 12.1). Once V_m reaches threshold, time- and voltage-dependent conductance changes occur in the active Na^+ and K^+ gates that drive V_m toward E_{Na}, then back to E_K, and finally to the resting potential. These changes in conductance were first described by Hodgkin and Huxley (and Katz as a coauthor on one paper and a collaborator on several others). Figure 12.19 illustrates a stylized action potential with the threshold potential at approximately −40 mV.

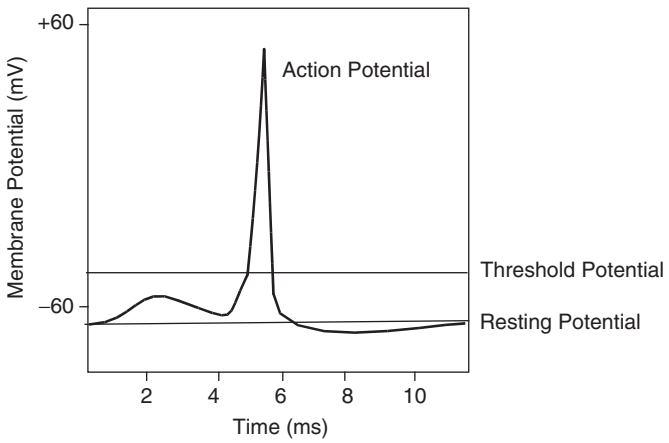

FIGURE 12.19 Stylized diagram of an action potential once threshold potential is reached at approximately 5 ms. The action potential is due to voltage and time-dependent changes in conductance. The action potential rise is due to Na^+, and the fall is due to K^+ conductance changes.

Stimulation of the postsynaptic membrane along the dendrite and cell body must occur for V_m to rise to the threshold potential at the axon hillock. As previously described, the greater the distance from the axon hillock, the smaller the contribution of postsynaptic membrane stimulation to the change in V_m at the axon hillock. Also, because of the membrane time constant, there is a time delay in stimulation at the postsynaptic membrane and the resultant change in V_m at the axon hillock. Thus, time and distance are important functions in describing the graded response of V_m at the axon hillock.

Once V_m reaches threshold, active Na^+ conductance gates are opened and an inward flow of Na^+ ions results, causing further depolarization. This depolarization increases Na^+ conductance, consequently inducing more Na^+ current. This iterative cycle, shown in Figure 12.20, continues driving V_m to E_{Na} and concludes with the closure of the Na^+ gates. A similar but slower change in K^+ conductance occurs that drives V_m back to the resting potential. Once an action potential is started, it continues until completion. This is called the "all or none" phenomenon. The active gates for Na^+ and K^+ are both functions of V_m and time.

The action potential moves through the axon at high speeds and appears to jump from one node of Ranvier to the next in myelinated neurons. This occurs because the membrane capacitance of the myelin sheath is very small, making the membrane appear only resistive with almost instantaneous changes in V_m possible.

To investigate the action potential, Hodgkin and Huxley used an unmyelinated squid giant axon in their studies because of its large diameter (up to 1 mm) and long survival time of several hours in seawater at 6.3°C. Their investigations examined the then existing theory that described an action potential as due to enormous changes in membrane permeability that allowed all ions to freely flow across the membrane, driving V_m to zero. As they discovered, this was not the case. The success of the Hodgkin-Huxley studies was based on two new experimental techniques, the space clamp and voltage clamp, and collaboration with Cole and Curtis from Columbia University.

The space clamp allowed Hodgkin and Huxley to produce a constant V_m over a large region of the membrane by inserting a silver wire inside the axon and thus eliminating R_a. The voltage clamp allowed the control of V_m by eliminating the effect of further depolarization due to the influx of I_{Na} and efflux of I_K as membrane permeability changed. Selection of the squid giant axon was fortunate for two reasons: it was large and survived a very long time in seawater, and it had only two types of voltage-time-dependent permeable channels. Other types of neurons have more than two voltage-time-dependent permeable channels that would have made the analysis extremely difficult or even impossible.

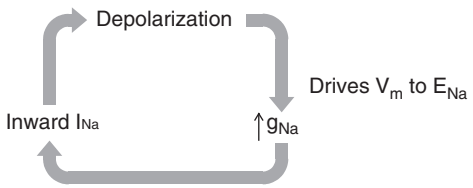

FIGURE 12.20 The conductance gate for sodium.

Voltage Clamps

To study the variable voltage-time-resistance channels for K^+ and Na^+, Hodgkin and Huxley used a voltage clamp to separate these two dynamic mechanisms so only the time-dependent features of the channel were examined. Figure 12.21 shows the voltage clamp experiment by using the equivalent circuit model previously described. The channels for K^+ and Na^+ are represented using variable voltage-time resistances, and the passive gates for Na^+, K^+, and Cl^- are given by a leakage channel with resistance R_l (that is, the Thevenin's equivalent circuit of the passive channels). The function of the voltage clamp is to suspend the interaction between Na^+ and K^+ channel resistance and the membrane potential, as shown in Figure 12.22. If the membrane voltage is not clamped, then changes in Na^+ and K^+ channel resistance modify membrane voltage, which then changes Na^+ and K^+ channel resistance, and so on, as previously described.

A voltage clamp is created by using two sets of electrodes, as shown in Figure 12.23. In an experiment, one pair injects current, I_m, to keep V_m constant, and another pair is used to observe V_m. To estimate the conductance in the Na^+ and K^+ channels, I_m is also measured during the experiment. Meters for recording V_m and I_m are shown in Figure 12.21. They

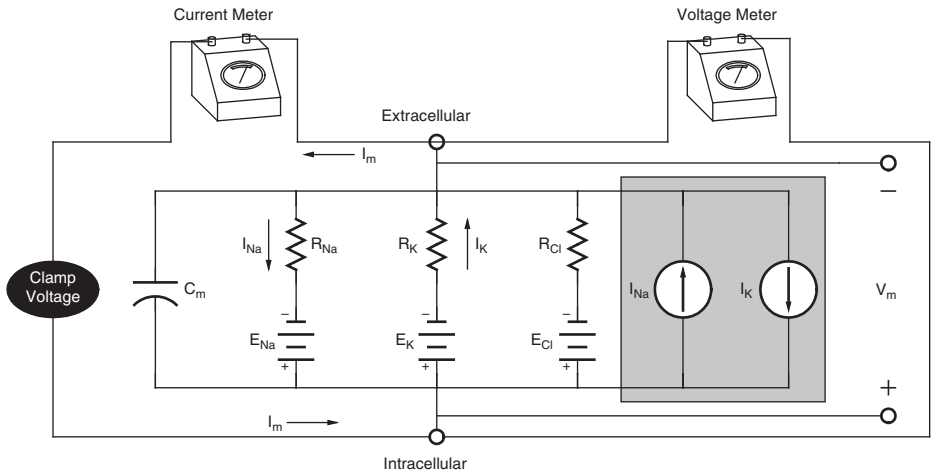

FIGURE 12.21 Equivalent circuit model of an unmyelinated section of squid giant axon under voltage clamp conditions. The channels for K^+ and Na^+ are now represented using variable voltage-time resistances, and the passive gates for Na^+, K^+, and Cl^- are given by a leakage channel with resistance R_l. The Na-K pump is illustrated within the shaded area of the circuit. In the experiment, the membrane is immersed in the seawater bath.

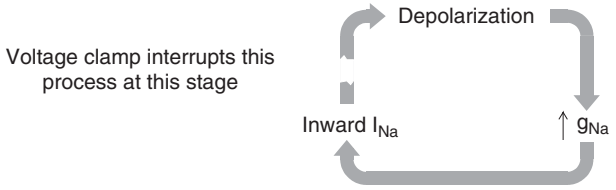

FIGURE 12.22 Voltage clamp experiment interrupts the cycle shown in Figure 12.20.

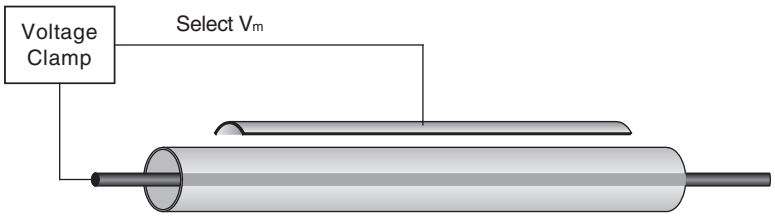

FIGURE 12.23 Physical set up for the voltage clamp experiment.

are placed outside the seawater bath. Today, these would be connected to an analog-to-digital converter (ADC) with data stored in a hard disk of a computer. Back in 1952, these meters were strip chart recorders. The application of a clamp voltage, V_c, causes a change in Na^+ conductance that results in an inward flow of Na^+ ions. This causes the membrane potential to be more positive than V_c. The clamp removes positive ions from inside the cell, which results in no net change in V_m. The current, I_m, is the dependent variable in the voltage clamp experiment, and V_c is the independent variable.

To carry out the voltage clamp experiment, the investigator first selects a clamp voltage and then records the resultant membrane current, I_m, that is necessary to keep V_m at the clamp voltage. Figure 12.24 shows the resulting I_m due to a clamp voltage of -20 mV. Initially, the step change in V_m causes a large current to pass through the membrane that is primarily due to the capacitive current. The clamp voltage also creates a constant leakage current through the membrane that is equal to

$$I_l = \frac{V_c - E_l}{R_l} \tag{12.38}$$

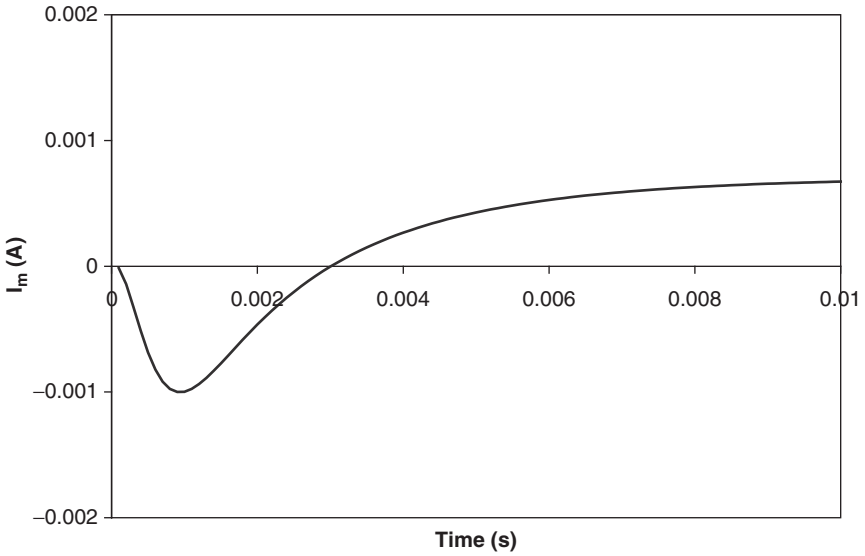

FIGURE 12.24 Membrane current I_m due to a -20 mV voltage clamp.

Subtracting both the capacitive and leakage current from I_m leaves only the Na^+ and K^+ currents. To separate the Na^+ and K^+ currents, Hodgkin and Huxley substituted a large impermeable cation for Na^+ in the external solution. This eliminated the Na^+ current and left only the K^+ current. Returning the Na^+ current to the external solution allowed the Na^+ current to be estimated by subtracting the capacitive, leakage, and K^+ currents from I_m. The Na^+ and K^+ currents due to a clamp voltage of -20 mV are shown in Figure 12.25. Since the clamp voltage in Figure 12.25 is above threshold, the Na^+ and K^+ channel resistances are engaged and follow a typical profile. The Na^+ current rises to a peak first and then returns to zero as the clamp voltage is maintained. The K^+ current falls to a steady-state current well after the Na^+ current peaks and is maintained at this level until the clamp voltage is removed. This general pattern holds for both currents for all clamp voltages above threshold.

The Na^+ and K^+ channel resistance or conductance is easily determined by applying Ohm's law to the circuit in Figure 12.20 and the current waveforms in Figure 12.21:

$$I_K = \frac{V_m - E_K}{R_K} = G_K(V_m - E_K) \tag{12.39}$$

$$I_{Na} = \frac{E_{Na} - V_m}{R_{Na}} = G_{Na}(E_{Na} - V_m) \tag{12.40}$$

These conductances are plotted as a function of clamp voltages ranging from -50 mV to $+20$ mV in Figure 12.26.

For all clamp voltages above threshold, the rate of onset for opening Na^+ channels is more rapid than for K^+ channels, and the Na^+ channels close after a period of time, while

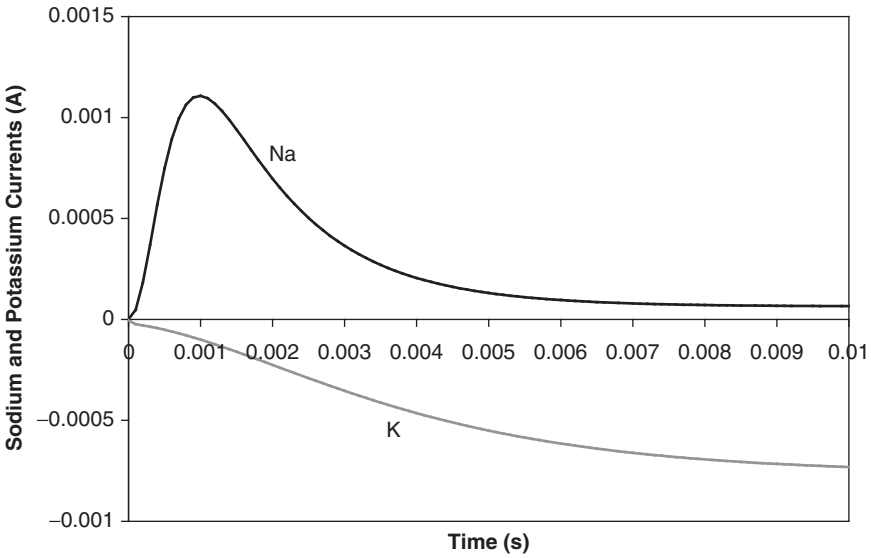

FIGURE 12.25 Diagram illustrating sodium and potassium currents due to a -20 mV voltage clamp.

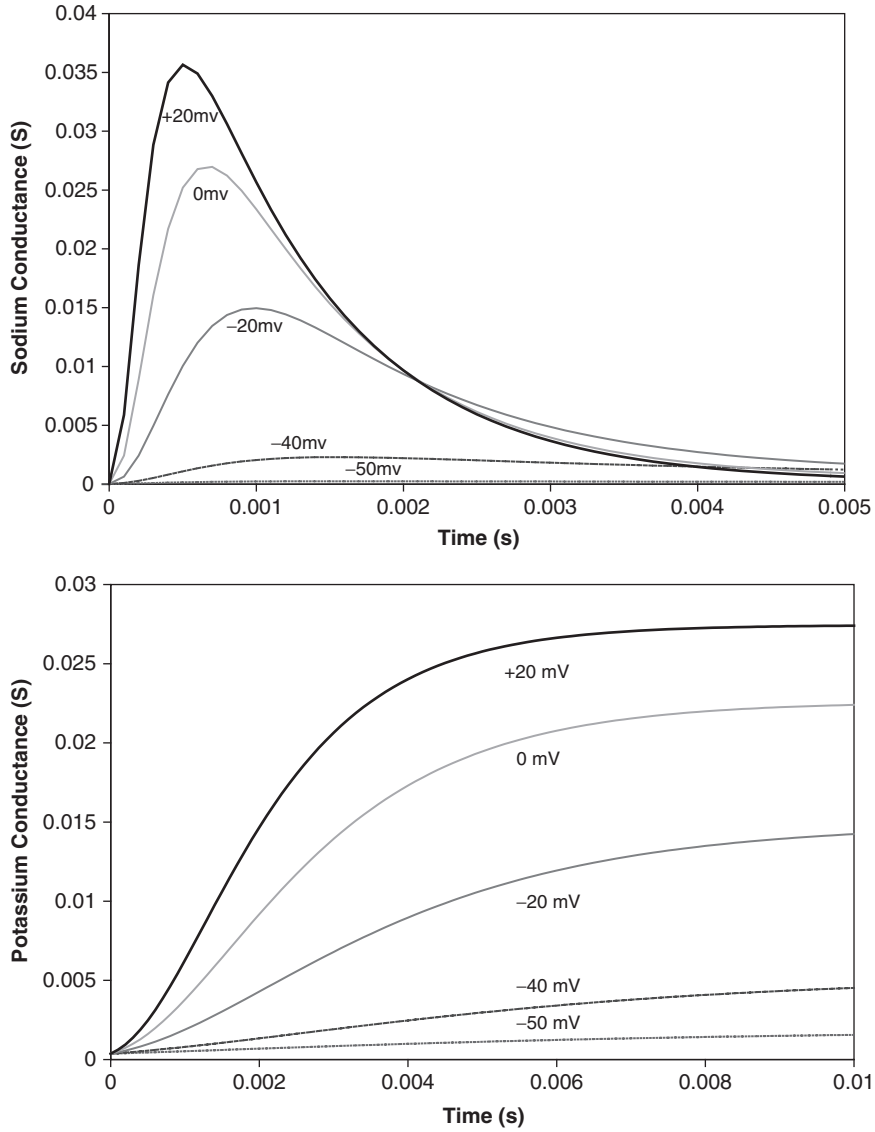

FIGURE 12.26 Diagram illustrating the change in Na^+ and K^+ conductance with clamp voltage ranging from −50 mV (below threshold) to +20 mV. Note that the time scales are different in the two conductance plots.

K^+ channels remain open while the voltage clamp is maintained. Once the Na^+ channels close, they cannot be opened until the membrane has been hyperpolarized to its resting potential. The time spent in the closed state is called the refractory period. If the voltage clamp is turned off before the time course for Na^+ is complete (returns to zero), G_{Na} almost immediately returns to zero, and G_K returns to zero slowly regardless of whether the time course for Na^+ is complete.

EXAMPLE PROBLEM 12.7

Compute I_c and I_l through a cell membrane for a subthreshold clamp voltage.

Solution

Assume that the Na^+ and K^+ voltage-time-dependent channels are not activated because the stimulus is below threshold. This eliminates these gates from the analysis although this is not actually true as shown in Example Problem 12.9. The cell membrane circuit is given by

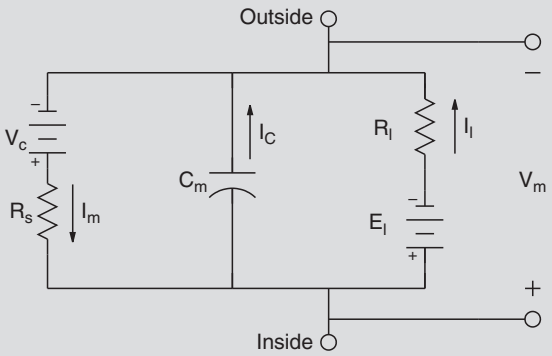

where R_s is the resistance of the wire. Applying Kirchhoff's current law at the cytoplasm gives

$$C_m \frac{dV_m}{dt} + \frac{V_m - E_l}{R_l} + \frac{V_m - V_c}{R_s} = 0$$

Rearranging the terms in the previous equation yields

$$C_m \frac{dV_m}{dt} + \frac{R_l + R_s}{R_l R_s} V_m = \frac{R_l V_c + R_s E_l}{R_l R_s}$$

With the initial condition $V_m(0) = E_l$, the solution is given by

$$V_m = \frac{R_l V_c + R_s E_l}{R_l + R_s} + \frac{R_l (E_l - V_c)}{R_l + R_s} e^{-\frac{(R_l + R_s)t}{R_l R_s C_m}}$$

Now

$$I_c = C_m \frac{dV_m}{dt} = \frac{E_l - V_c}{R_s} e^{-\frac{(R_l + R_s)t}{R_l R_s C_m}}$$

and $I_l = \dfrac{V_m - E_l}{R_l}$. At steady-state, $I_l = \dfrac{V_c - E_l}{R_l + R_s}$.

Reconstructing the Action Potential

By analyzing the estimated G_{Na} and G_K from voltage clamp pulses of various amplitudes and durations, Hodgkin and Huxley were able to obtain a complete set of nonlinear empirical equations that described the action potential. Simulations using these

equations accurately describe an action potential in response to a wide variety of stimulations. Before presenting these equations, it is important to qualitatively understand the sequence of events that occur during an action potential by using previously described data and analyses. The start of an action potential begins with a depolarization above threshold that causes an increase in G_{Na} and results in an inward Na^+ current. The Na^+ current causes a further depolarization of the membrane, which then increases the Na^+ current. This continues to drive V_m to the Nernst potential for Na^+. As shown in Figure 12.26, G_{Na} is a function of both time and voltage, which peaks and then falls to zero.

During the time it takes for G_{Na} to return to zero, G_K continues to increase, which hyperpolarizes the cell membrane and drives V_m from E_{Na} toward E_K. The increase in G_K results in an outward K^+ current. The K^+ current causes further hyperpolarization of the membrane, which then increases K^+ current. This continues to drive V_m to the Nernst potential for K^+, which is below resting potential. Figure 12.27 illustrates the changes in V_m, G_{Na}, and G_K during an action potential.

The circuit shown in Figure 12.16 is a useful tool for modeling the cell membrane during small subthreshold depolarizations. This model assumes that the K^+ and Na^+ currents are small enough to neglect. As illustrated in Example Problem 12.6, a current pulse sent through the cell membrane briefly creates a capacitive current, which decays exponentially and creates an exponentially increasing I_l. Once the current pulse is turned off, capacitive current flows again and exponentially decreases to zero. The leakage current also exponentially decays to zero.

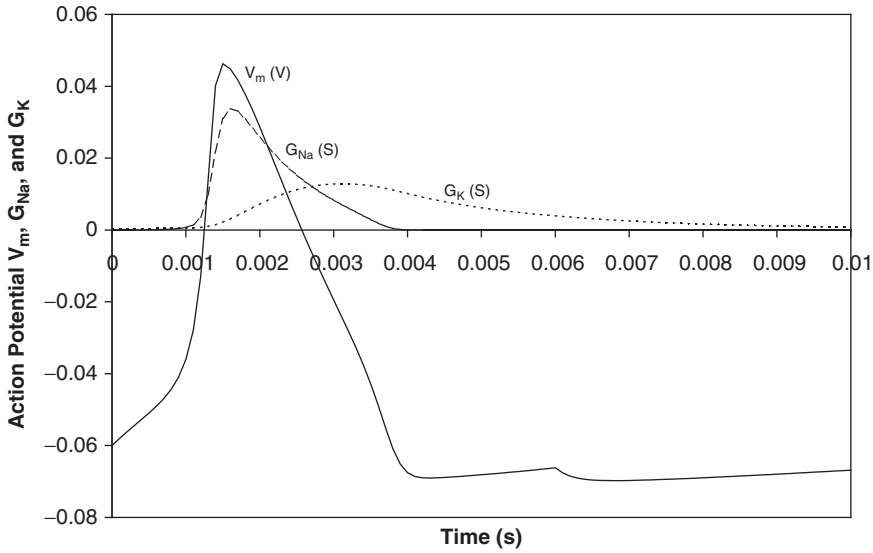

FIGURE 12.27 V_m, G_{Na}, and G_K during an action potential.

As the current pulse magnitude is increased, depolarization of the membrane increases, causing activation of the Na^+ and K^+ voltage-time-dependent channels. For sufficiently large depolarizations, the inward Na^+ current exceeds the sum of the outward K^+ and leakage currents ($I_{Na} > I_K + I_l$). The value of V_m at this current is called *threshold*. Once the membrane reaches threshold, the Na^+ and K^+ voltage-time channels are engaged and run to completion, as shown in Figure 12.27.

If a slow rising stimulus current is used to depolarize the cell membrane, then threshold will be higher. During the slow approach to threshold, inactivation of G_{Na} channels occurs and activation of G_K channels develops before threshold is reached. The value of V_m, where $I_{Na} > I_K + I_l$ is satisfied, is much larger than if the approach to threshold occurs quickly.

12.6.2 Equations Describing G_{Na} and G_K

The empirical equation used by Hodgkin and Huxley to model G_{Na} and G_K is of the form

$$G(t) = \left(A + Be^{-Ct}\right)^D \tag{12.41}$$

Values for the parameters $A, B, C,$ and D were estimated from the voltage clamp data that were collected on the squid giant axon. Not evident in Eq. (12.41) is the voltage dependence of the conductance channels. The voltage dependence is captured in the parameters as described in this section. In each of the conductance models, D is selected as 4 to give a best fit to the data. Figure 12.27 was actually calculated using SIMULINK, a simulation package that is part of MATLAB, and the parameter estimates found by Hodgkin and Huxley. Details concerning the simulation are covered later in this section.

Potassium

The potassium conductance waveform shown in Figure 12.26 is described by a rise to a peak while the stimulus is applied. This aspect is easily included in a model of G_K by using the general Hodgkin-Huxley expression as follows.

$$G_K = \bar{G}_K n^4 \tag{12.42}$$

where $\bar{G}_K$ is maximum K^+ conductance and n is thought of as a rate constant and given as the solution to the following differential equation:

$$\frac{dn}{dt} = \alpha_n(1 - n) - \beta_n n \tag{12.43}$$

where

$$\alpha_n = 0.01\frac{V+10}{e^{\frac{V+10}{10}}-1}$$

$$\beta_n = 0.125e^{\frac{V}{80}}$$

$$V = V_{rp} - V_m$$

V_{rp} is the membrane potential at rest without any membrane stimulation. Note that V is the displacement from resting potential and should be negative. Clearly, G_K is a time-dependent variable, since it depends on Eq. (12.43), and a voltage-dependent variable, since n depends on voltage because of α_n and β_n.

Sodium

The sodium conductance waveform in Figure 12.26 is described by a rise to a peak and a subsequent decline. These aspects are included in a model of G_{Na} as the product of two functions, one describing the rising phase and the other describing the falling phase, and modeled as

$$G_{NA} = \bar{G}_{Na}m^3h \tag{12.44}$$

where $\bar{G}_{Na}$ is maximum Na^+ conductance, and m and h are thought of as rate constants and given as the solutions to the following differential equations:

$$\frac{dm}{dt} = \alpha_m(1-m) - \beta_m m \tag{12.45}$$

where

$$\alpha_m = 0.1\frac{V+25}{e^{\frac{V+25}{10}}-1}$$

$$\beta_m = 4e^{\frac{V}{18}}$$

and

$$\frac{dh}{dt} = \alpha_h(1-h) - \beta_h h \tag{12.46}$$

where

$$\alpha_h = 0.07e^{\frac{V}{20}}$$

$$\beta_h = \frac{1}{e^{\frac{V+30}{10}}+1}$$

Note that m describes the rising phase and h describes the falling phase of G_{Na}. The units for the $\alpha_i's$ and $\beta_i's$ in Eqs. (12.43), (12.45), and (12.46) are ms^{-1}, while n, m, and h are dimensionless and range in value from 0 to 1.

EXAMPLE PROBLEM 12.8

Calculate G_K and G_{Na} at resting potential for the squid giant axon using the Hodgkin-Huxley model. Parameter values are $\bar{G}_K = 36 \times 10^{-3}$ S and $\bar{G}_{Na} = 120 \times 10^{-3}$ S.

Solution

At resting potential, G_K and G_{Na} are constant with values dependent on n, m, and h. Since the membrane is at steady state, $\frac{dn}{dt} = 0$, $\frac{dm}{dt} = 0$, and $\frac{dh}{dt} = 0$. Using Eqs. (12.43), (12.45), and (12.46), at resting potential and steady state

$$n = \frac{\alpha_n^0}{\alpha_n^0 + \beta_n^0}$$

$$m = \frac{\alpha_m^0}{\alpha_m^0 + \beta_m^0}$$

$$h = \frac{\alpha_h^0}{\alpha_h^0 + \beta_h^0}$$

where α_i^0 is α at $V = 0$ for $i = n, m,$ and h, and β_i^0 is β at $V = 0$ for $i = n, m,$ and h. Calculations yield $\alpha_n^0 = 0.0582$, $\beta_n^0 = 0.125$, $n = 0.31769$, $\alpha_m^0 = 0.2236$, $\beta_m^0 = 4$, $m = 0.05294$, $\alpha_h^0 = 0.07$, $\beta_h^0 = 0.04742$, and $h = 0.59615$. Therefore, at resting potential and steady state

$$G_K = \bar{G}_K n^4 = 36.0 \times 10^{-3} (0.31769)^4 = 0.3667 \times 10^{-3} \text{ S}$$

and

$$G_{Na} = \bar{G}_{Na} m^3 h = 120.0 \times 10^{-3} (0.05294)^3 \times 0.59615 = 0.010614 \times 10^{-3} \text{ S}$$

12.6.3 Equation for the Time Dependence of the Membrane Potential

Figure 12.28 shows a model of the cell membrane that is stimulated via an external stimulus, I_m, which is appropriate for simulating action potentials. Applying Kirchhoff's current law at the cytoplasm yields

$$I_m = G_K(V_m - E_K) + G_{Na}(V_m - E_{Na}) + \frac{(V_m - E_l)}{R_l} + C_m \frac{dV_m}{dt} \tag{12.47}$$

where G_K and G_{Na} are the voltage-time dependent conductances given by Eqs. (12.42) and (12.44).

EXAMPLE PROBLEM 12.9

For the squid giant axon, compute the size of the current pulse (magnitude and pulse width) necessary to raise the membrane potential from its resting value of −60 mV to −40 mV and then back to its resting potential. Neglect any changes in K^+ and Na^+ conductances from resting potential, but include G_K and G_{Na} at resting potential in the analysis. Hodgkin-Huxley parameter values

Continued

for the squid giant axon are $G_l = \dfrac{1}{R_l} = 0.3 \times 10^{-3}$ S, $\bar{G}_K = 36 \times 10^{-3}$ S, $\bar{G}_{Na} = 120 \times 10^{-3}$ S, $E_K = -72 \times 10^{-3}$V, $E_l = -49.4 \times 10^{-3}$V, $E_{Na} = 55 \times 10^{-3}$V, and $C_m = 1 \times 10^{-6}$F.

Solution

Let current I_m be given by $I_m = K(u(t) - u(t - t_0))$. In Example Problem 12.8, the conductances at resting potential were calculated as $G_K = 0.3667 \times 10^{-3}$ S and $G_{Na} = 0.010614 \times 10^{-3}$ S. Since G_K and G_{Na} remain constant for a subthreshold current stimulus in this problem, the circuit in Figure 12.28 reduces to the following circuit. For ease in analysis, this circuit is replaced by the following Thevenin's equivalent circuit with

$$R_{Th} = \frac{1}{G_{Na} + G_K + G_l} = 1.4764\ k\Omega$$

and

$$V_{TH} = -60\ \text{mV}.$$

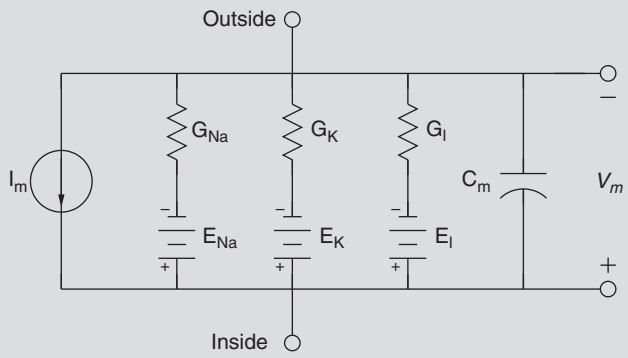

Since the solution in Example Problem 12.6 is the same as the solution in this problem, we have

$$V_m(t) = V_{TH} + R_{TH}K\left(1 - e^{-\frac{t}{R_{TH}C_m}}\right)u(t) - R_{TH}K\left(1 - e^{-\frac{t-t_o}{R_{TH}C_m}}\right)u(t - t_0)$$

For convenience, assume the current pulse $t_0 > 5\tau$. Therefore, for $5\tau < t \leq t_o$, $V_m = -40$ mV according to the problem statement at steady state, and from the preceding equal, V_m reduces to

$$V_m = -0.040 = V_{TH} + K \times R_{TH} = -0.06 + K \times 1476.4$$

which yields $K = 13.6\ \mu$A. Since $\tau = R_{TH}C_m = 1.47$ ms, any value for t_0 greater than $5\tau = 7.35$ ms brings V_m to -40 mV with $K = 13.6\ \mu$A. Naturally, a larger current pulse magnitude is needed for an action potential because as V_m exponentially approaches threshold (reaching it with a duration of infinity), the Na^+ conductance channels become inactive and shut down.

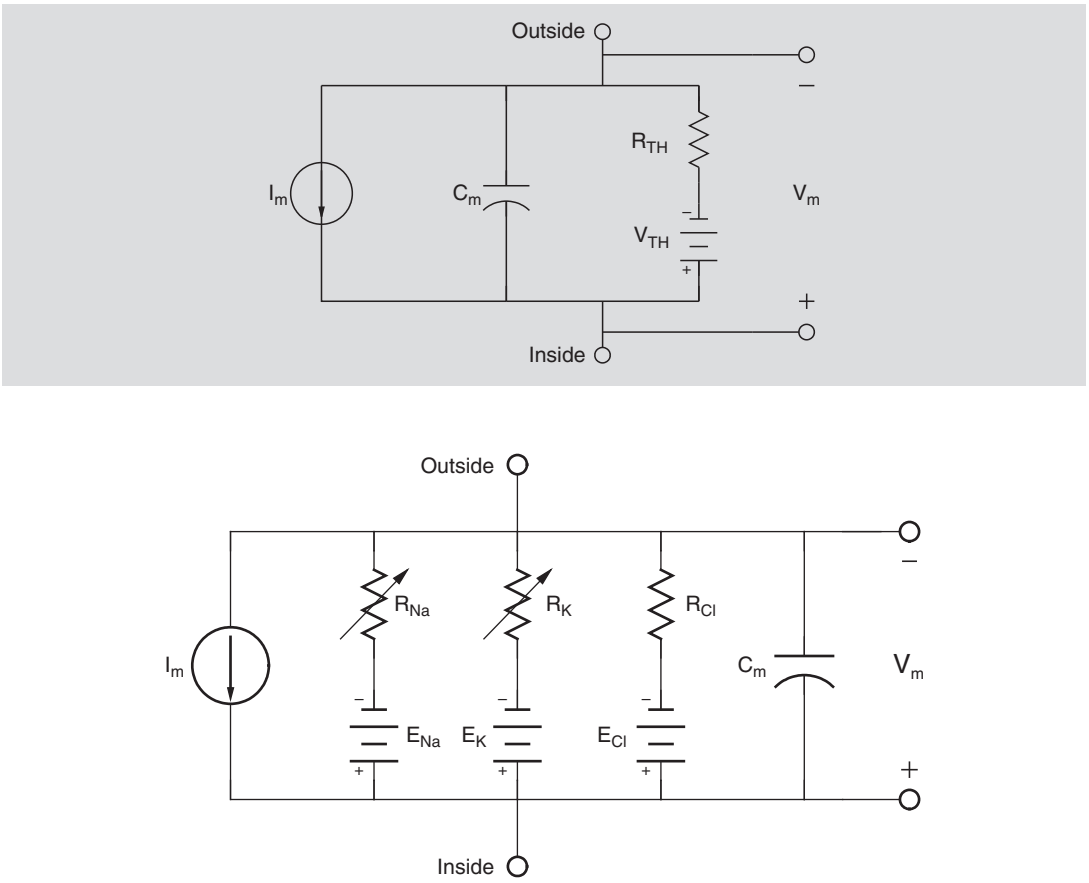

FIGURE 12.28 Circuit model of an unmyelinated section of squid giant axon. The channels for K^+ and Na^+ are represented using the variable voltage-time conductances given in Eqs. (12.42) and (12.44). The passive gates for Na^+, K^+, and Cl^- are given by a leakage channel with resistance, R_l, and Nernst potential, E_l. The *Na-K* pump is not drawn for ease in analysis, since it does not contribute any current to the rest of the circuit.

To find V_m during an action potential, four differential equations (Eqs. (12.43), (12.45), (12.46), and (12.47)) and six algebraic equations ($\alpha_i's$ and $\beta_i's$ in Eqs. (12.43), (12.45), and (12.46)) need to be solved. Since the system of equations is nonlinear due to the n^4 and m^3 conductance terms, an analytic solution is not possible. To solve for V_m, it is therefore necessary to simulate the solution. There are many computer tools that allow a simulation solution of nonlinear systems. SIMULINK, a general purpose toolbox in MATLAB that simulates solutions for linear and nonlinear, continuous, and discrete dynamic systems, is used in this textbook. SIMULINK is a popular and widely used simulation program with a user-friendly interface that is fully integrated within MATLAB. SIMULINK is interactive and works on most computer platforms. Analogous to an analog computer, programs for SIMULINK are developed based on a block diagram of the system.

The SIMULINK program for an action potential is shown in Figures 12.29 to 12.32. The block diagram is created by solving for the highest derivative term in Eq. (12.47), which yields Eq. (12.48). The SIMULINK program is then created by using integrators, summers, and so on.

$$\frac{dV_m}{dt} = \frac{1}{C_m}(I_m + G_K(E_K - V_m) + G_{Na}(E_{Na} - V_m) + G_l(E_l - V_m)) \tag{12.48}$$

Figure 12.25 shows the main block diagram. Figures 12.29 to 12.31 are subsystems that were created for ease in analysis. The Workspace output blocks were used to pass simulation results to MATLAB for plotting. Parameter values used in the simulation were based on the empirical results from Hodgkin and Huxley, with $G_l = \frac{1}{R_l} = 0.3 \times 10^{-3}$ S, $\bar{G}_K = 36 \times 10^{-3}$ S, $\bar{G}_{Na} = 120 \times 10^{-3}$ S, $E_K = -72 \times 10^{-3}$ V, $E_l = -49.4 \times 10^{-3}$ V, $E_{Na} = 55 \times 10^{-3}$ V,

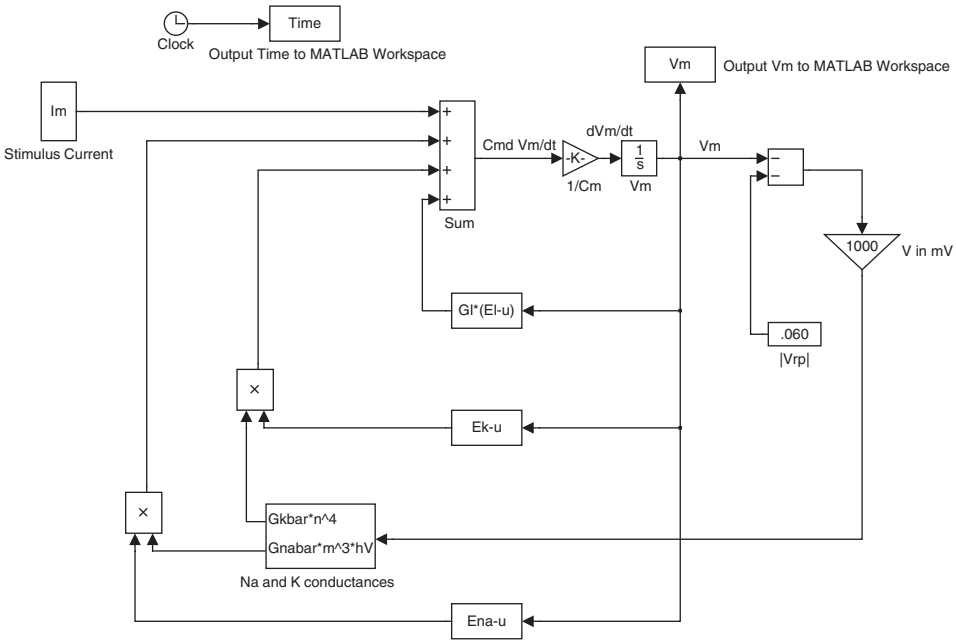

FIGURE 12.29 Main block diagram for simulating an action potential using SIMULINK. The stimulus current is a pulse created by subtracting two step functions as described in Figure 12.30. The Na^+ and K^+ conductance function blocks are described in Figures 12.31 and 12.32.

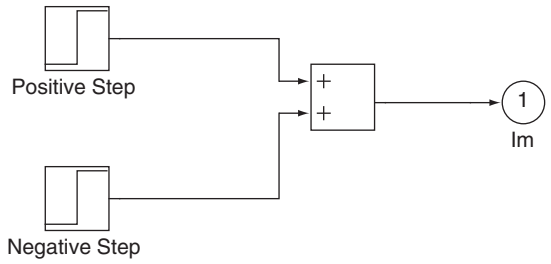

FIGURE 12.30 The stimulus current.

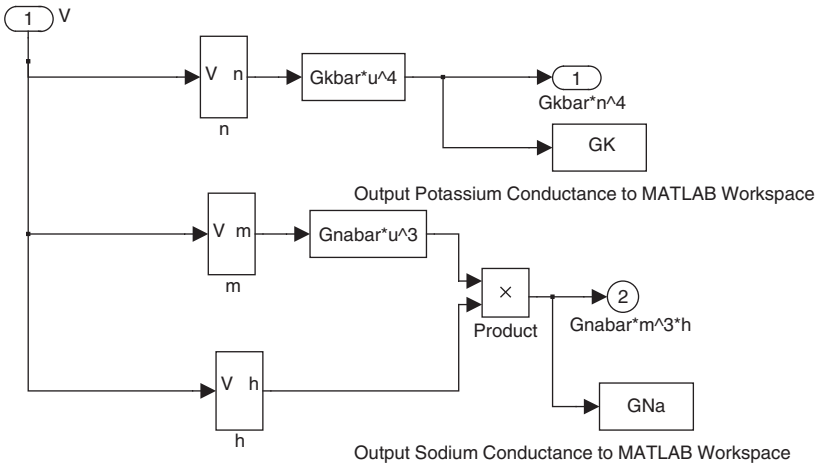

FIGURE 12.31 SIMULINK program for the K^+ and Na^+ conductance channels.

and $C_m = 1 \times 10^{-6}$ F. Figure 12.23 is a SIMULINK simulation of an action potential. The blocks Gl*(El-u), Ek-u, and Ena-u are function blocks that were used to represent the terms $G_l\,(E_l - V_m)$, $(E_{\mathrm{K}} - V_m)$, and $(E_{\mathrm{Na}} - V_m)$ in Eq. (12.48), respectively.

The stimulus pulse current was created by using the SIMULINK step function as shown in Figure 12.30. The first step function starts at $t = 0$ with magnitude K, and the other one starts at $t = t_0$ with magnitude $-K$. The current pulse should be sufficient to quickly bring V_{m} above threshold.

Figure 12.31 illustrates the SIMULINK program for the conductance channels for Na^+ and K^+. Function blocks Gkbar*u^4, Gnabar*u^3, and Gnabar*m^3*h represent $\bar{G}_K\ n^4$, $\bar{G}_{Na}\ m^3$, and $\bar{G}_{Na}\ m^3h$, respectively. The subsystems n, m, and h are described in Figure 12.32 and are based on six algebraic equations for α_i's and β_i's in Eqs. (12.43), (12.45), and (12.46).

12.7 MODEL OF A WHOLE NEURON

This section brings together the entire neuron, combing the dendrite, soma, axon, and presynaptic terminal. Dendrites and axons can be modeled as a series of cylindrical compartments, each connected together with an axial resistance, as described in Section 12.5.3. Both the axon and dendrites are connected to the soma. Of course, real neurons have many different arrangements, such as the dendrite connected to the axon, which then connects to the soma. The basic neuron consists of many dendrites, one axon, and one soma. Note that the dendrite and axon do not have to have constant diameter cylinders but may narrow toward the periphery.

As described previously, Figure 12.17 illustrates a generic electrical dendrite compartment model with passive channels, and Figure 12.28 illustrates the axon compartment with active channels at the axon hillock and the node of Ranvier. To model the myelinated portion of the axon, a set of passive compartments, like the dendrite compartment, can be used with capacitance, passive ion channels, and axial resistance. Shown in Figure 12.33 is a portion of the axon with myelin sheath, with three passive channels, and an active component

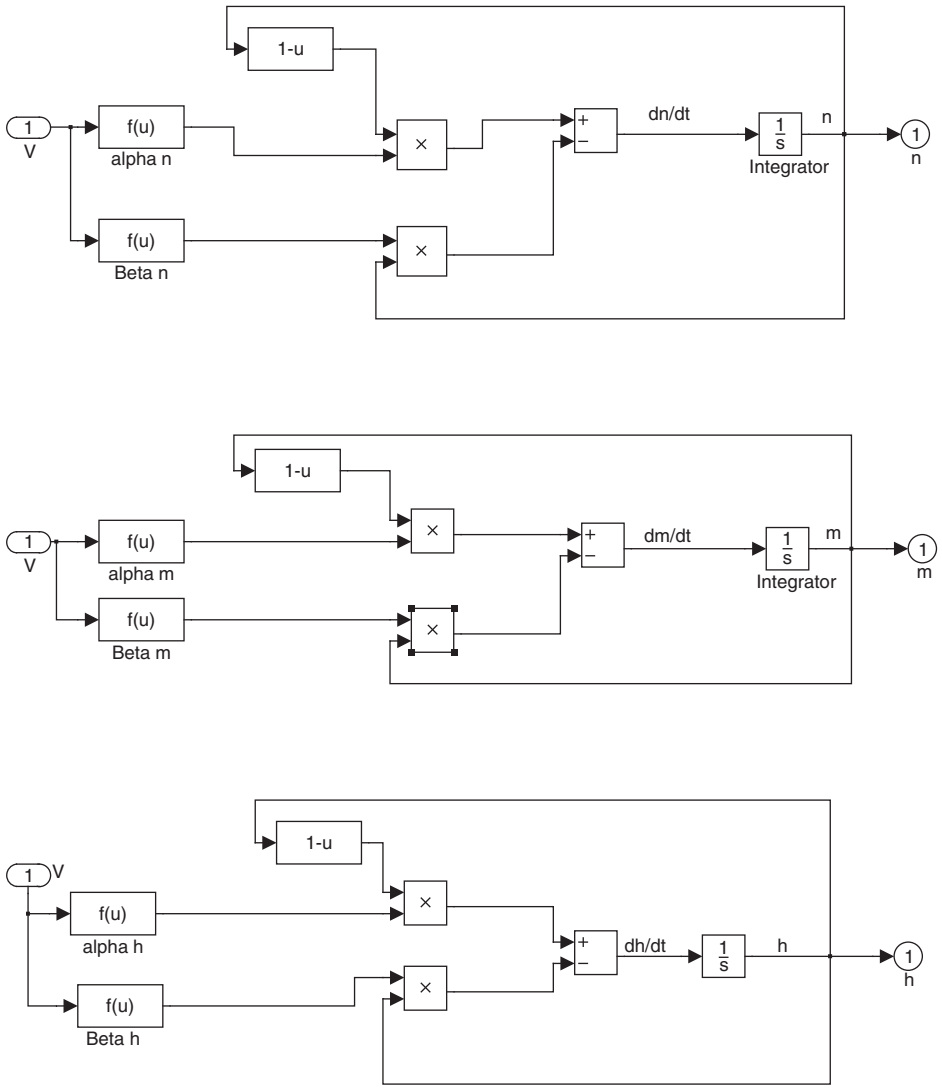

FIGURE 12.32 SIMULINK program for the alpha and beta terms in Equations (12.43), (12.45) and (12.46).

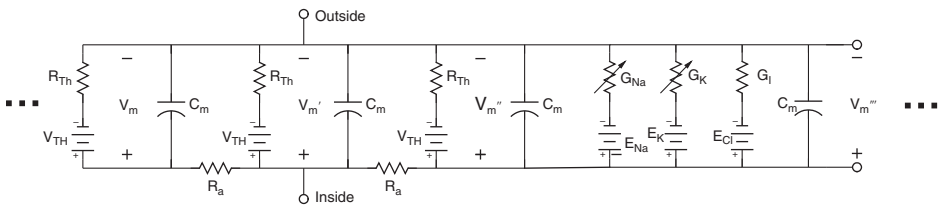

FIGURE 12.33 A segment of the axon with active and passive compartments.

for the node of Ranvier. The structure in Figure 12.33 can be modified for any number of compartments as appropriate. The soma can be modeled as an active or passive compartment depending on the type of neuron.

To model the neuron in Figure 12.33, Kirchhoff's current law is applied for each compartment (i.e., each line in Eq. (12.49) is for a compartment), giving

$$\begin{aligned}
&\ldots + C_m \frac{dV_m}{dt} + \frac{(V_m - V_{TH})}{R_{TH}} + \frac{(V_m - V'_m)}{R_a} \\
&+ C_m \frac{dV'_m}{dt} + \frac{(V'_m - V_{TH})}{R_{TH}} + \frac{(V'_m - V''_m)}{R_a} \\
&+ C_m \frac{dV''_m}{dt} + \frac{(V''_m - V_{TH})}{R_{TH}} + \frac{(V''_m - V'''_m)}{R_a} \\
&+ G_K(V'''_m - E_K) + G_{Na}(V'''_m - E_{Na}) + \frac{(V'''_m - E_l)}{R_l} + C_m \frac{dV'''_m}{dt} + \ldots
\end{aligned} \tag{12.49}$$

Because neurons usually have other channels in addition to the three of the squid giant axon, a model of the neuron should have the capability of including other channels, such as a fast sodium channel, delayed potassium conductance, high threshold calcium conductance, and so forth. Additional ion channels can be added for each compartment in Eq. (12.49) by adding

$$\sum_{i=1}^{n} G_i(V_m - E_i)$$

for each compartment for channels $i = 1, n$. The values of $C_m, R_{TH}, R_a,$ and G_i are dependent on the size of the compartment and the type of neuron modeled.

A complete model of the neuron can be constructed by including as many dendritic branches as needed, each described using Figure 12.17 and each modeled by

$$\ldots + C_m \frac{dV_m}{dt} + \frac{(V_m - V_{TH})}{R_{TH}} + \frac{(V_m - V'_m)}{R_a} + C_m \frac{dV'_m}{dt} + \frac{(V'_m - V_{TH})}{R_{TH}} + \frac{(V'_m - V''_m)}{R_a} + \ldots \tag{12.50}$$

a soma with passive or active properties using either

$$C_m \frac{dV_m}{dt} + \frac{(V_m - V_{TH})}{R_{TH}} + \frac{(V_m - V'_m)}{R_a} \tag{12.51}$$

or

$$G_K\left(V'''_m - E_K\right) + G_{Na}\left(V'''_m - E_{Na}\right) + \frac{(V'''_m - E_l)}{R_l} + C_m \frac{dV'''_m}{dt} \tag{12.52}$$

and an axon using Eq. (12.49) as described in Rodriguez and Enderle [3]. Except for the terminal compartment, two inputs are needed for the dendrite compartment: the input defined by the previous compartment's membrane potential and the next compartment's

membrane potential. Additional neurons can be added using the same basic neuron, interacting with each other using the current from the adjacent neuron (presynaptic terminal) to stimulate the next neuron.

For illustration purposes, the interaction between two adjacent neurons is modeled using SIMULINK, shown in Figure 12.34, and the results shown in Figure 12.35. Three voltage-dependent channels for Na^{+}, K^{+}, and Ca^{+2}, and also a leakage channel are used for the axon. We use a myelinated axon with four passive compartments between each node of Ranvier. The total axon consists of three active compartments and two myelinated passive segments. The dendrite consists of five passive compartments, and the soma is a passive spherical compartment. The stimulus is applied at the terminal end of the dendrite of the first neuron. It is modeled as an active electrode compartment. The size of each axon compartment is the same but different than the dendrite compartment. The input to the first neuron is shown in Figure 12.36.

12.8 CHEMICAL SYNAPSES

The previous section describes the movement of a signal through a change in membrane potential from the dendrite, soma, and axon to the presynaptic terminal. In this section, we examine the process that occurs at the presynaptic terminal, called the presynaptic neuron, and the interaction with the postsynaptic terminal on an adjacent neuron's dendrite, called the postsynaptic neuron. The major action in the communication between two adjacent neurons is the movement of a neurotransmitter from the presynaptic terminal to the postsynaptic terminal via diffusion, transferring electrical energy to chemical energy, and then back into electrical energy.

Another type of synapse is the gap junction that connects two neurons. Under this arrangement, ions move directly from one cell to the other. Since this form of communication is rather rare among neurons, we will not cover it any further here. Gap junctions are typically observed in signaling among smooth muscle fibers.

More than 40 neurotransmitters have been discovered, some that are excitatory and others that are inhibitionary. An example of an excitatory neurotransmitter is acetylcholine (ACh), which depolarizes the postsynaptic neuron's dendrite by opening sodium channels. An example of an inhibitionary neurotransmitter is gamma-aminobutyric acid (GABA), which opens the chloride channels that then hyperpolarizes the postsynaptic neuron's dendrite.

Figure 12.3 shows a set of converging presynaptic terminals on the postsynaptic neuron's dendritic membrane. The space between the two is called the synaptic gap. The distance between the two neurons is quite small and ranges from 200 to 500 angstroms. Important features in this form of communication is that it is one-way and analog, which allow for the summing of all asynchronous inputs. This one-way communication allows a precise communication and control among neurons with signals going in one direction only. Keep in mind that the gap junction is not a one-way communication channel, as it allows ions to move in either direction. It should also be noted that a small percentage of presynaptic terminals also converge on the soma, which eliminates the change in membrane potential as a function of distance that occurs on the dendrite.

Figure 12.37 depicts a single presynaptic terminal (top) and the postsynaptic terminal (bottom). The neurotransmitter is stored in numerous vesicles in the presynaptic neuron,

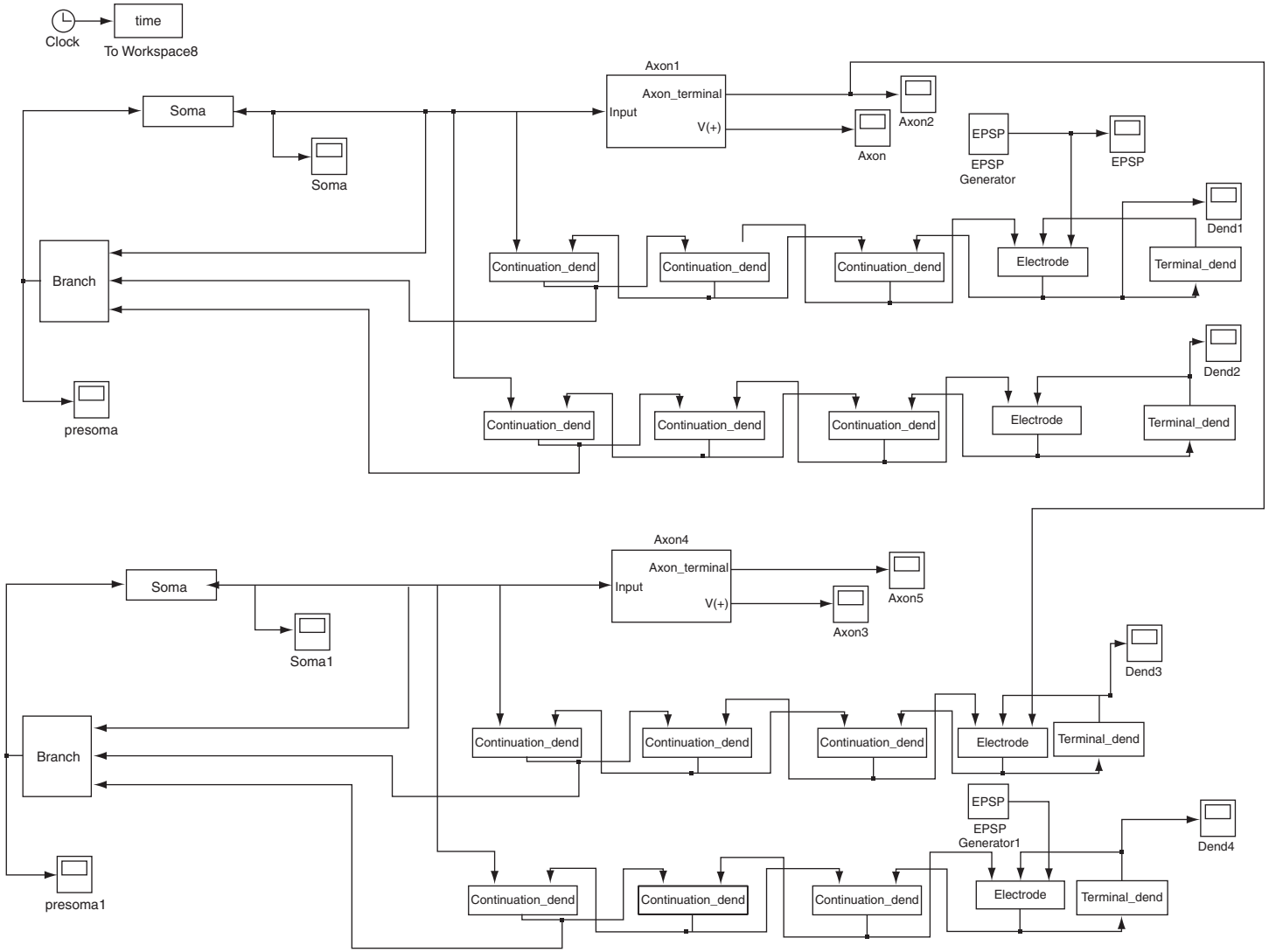

FIGURE 12.34 SIMULINK model for two adjacent neurons.

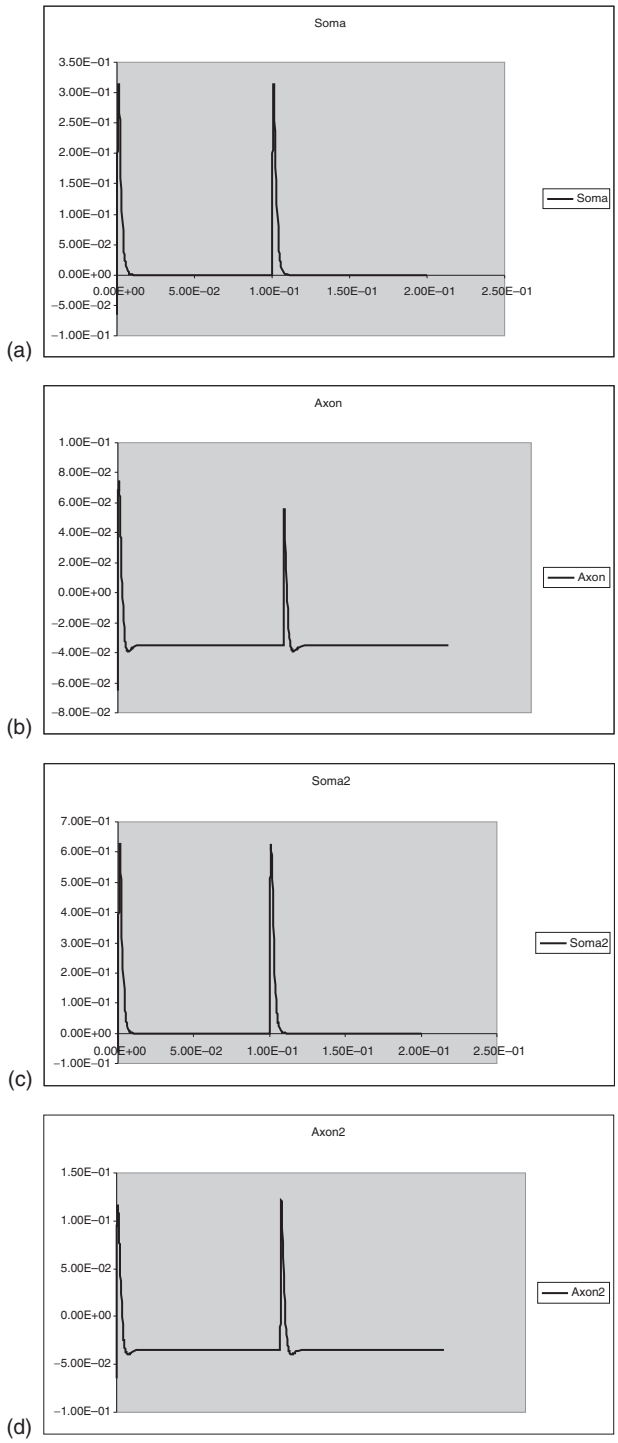

FIGURE 12.35 (a) Soma of first neuron, (b) axon of first neuron, (c) soma of second neuron, and (d) axon of second neuron.

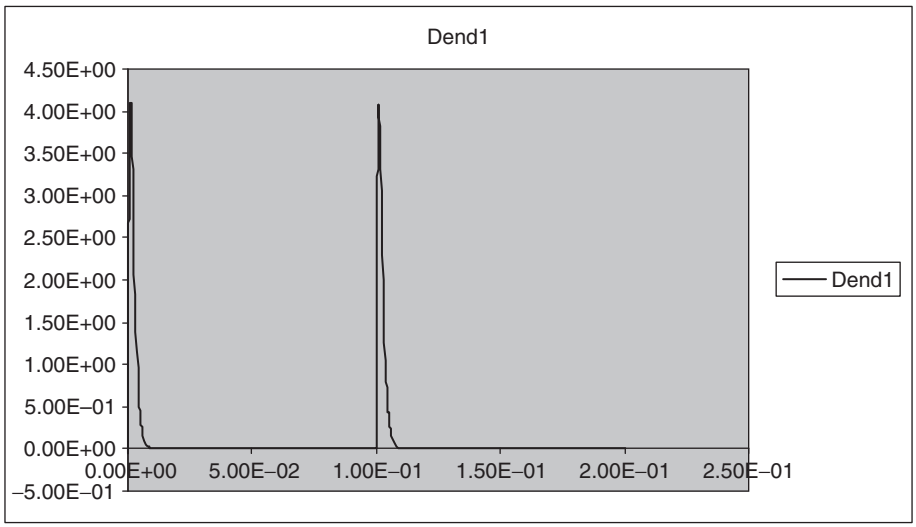

FIGURE 12.36 The stimulus to the first neuron.

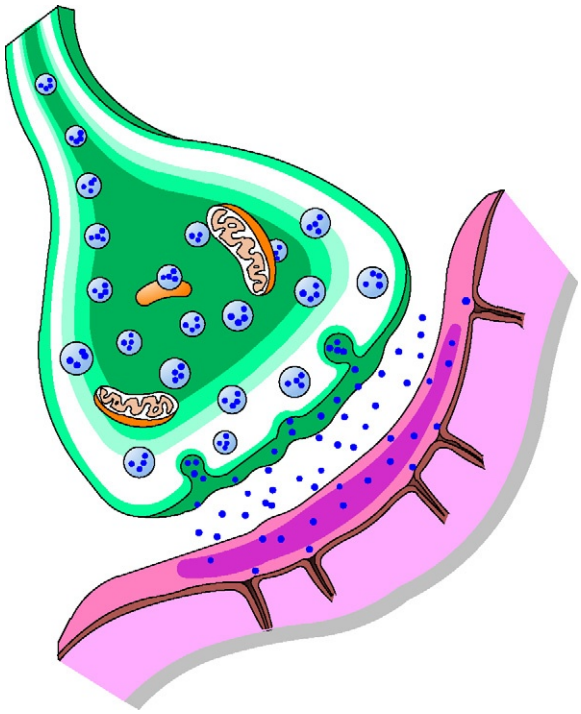

FIGURE 12.37 Presynaptic (top) and postsynaptic (bottom) terminals illustrating a neurotransmitter moving across the synaptic gap.

enough for responding to thousands of action potentials, where each vesicle stores approximately 10,000 molecules of neurotransmitter in vesicles. The mitochondria supplies ATP to resupply the vesicles with the neurotransmitter. The resupplying of the neurotransmitter into the vesicles occurs even while the presynaptic neuron is delivering the neurotransmitter into the synaptic gap during an action potential.

After an action potential reaches the presynaptic terminal, it depolarizes the membrane and causes the movement of a few vesicles toward the membrane. Once in the vicinity of the membrane, the vesicles then fuse with the membrane, as shown in Figure 12.38. This process usually occurs in less than 1 ms. The fused vesicle then opens and the neurotransmitter is released into the synaptic gap. This movement is not highly synchronized but occurs in a random fashion. After moving through the synaptic gap by diffusion, the neurotransmitter binds to a receptor in the postsynaptic neuron. The binding of the neurotransmitter to the postsynaptic receptor causes a change in membrane potential, either depolarization by an excitatory neurotransmitter, or hyperpolarization by an inhibitionary neurotransmitter. This process usually occurs in less than 1 ms.

Note that there are a large number of presynaptic terminals (10,000 to 200,000) that converge on the dendrite of a postsynaptic neuron. Each molecule of neurotransmitter causes a change in membrane potential, which all sum according to superposition as described in Example Problem 12.6. Note that synchronization is not essential because of the capacitive nature of the membrane. The change in membrane potential at the postsynaptic dendrite then travels to the soma as described in Section 12.5. If at the axon hillock the membrane potential crosses threshold, an action potential is created that then moves without attenuation down the axon, where the process repeats itself. If the membrane potential does not reach threshold at the axon hillock, it then returns to the steady-state resting potential.

12.8.1 Calcium Ions

While the exact mechanism for the movement of the neurotransmitter vesicles to the presynaptic terminal membrane and its release into the synaptic gap is unknown, it is believed to involve voltage-gated calcium ion channels. The concentration of Ca^{+2} is kept quite low in the cytosol during periods of rest. When an action potential arrives at the presynaptic

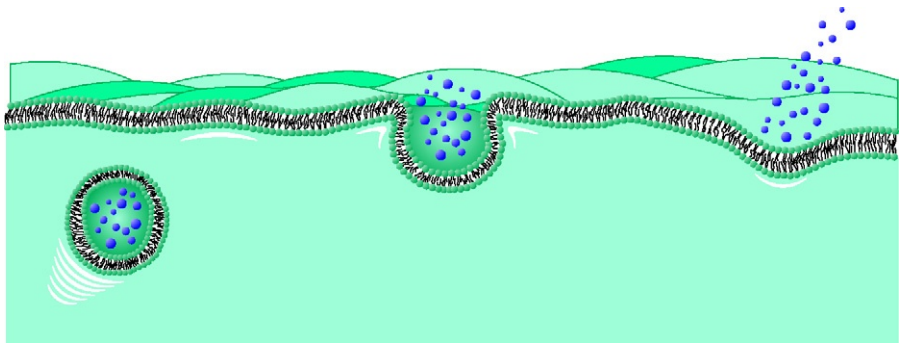

FIGURE 12.38 The movement of the vesicle through the cytosol to the cell membrane, where it fuses and then releases the neurotransmitter in the synaptic gap.

terminal, the concentration of Ca^{+2} in the cytosol quickly rises. The amount of Ca^{+2} in the cytosol appears to be proportional to the number of action potentials, and in turn, the amount of neurotransmitter released.

Keener and Sneyd [2] provide an excellent summary in Chapter 7 of the various theories involving the role of Ca^{+2} in the release of neurotransmitter into the synaptic gap. Two current models involve different roles for the change in membrane potential, one indicating that it has a direct effect on the amount of neurotransmitter released, and the other acting directly on the Ca^{+2} entering the cytosol.

For illustrative purposes, consider a model for the movement of the neurotransmitter vesicles that involves the transport of Ca^{+2} across the cell membrane using a carrier-mediated transport process as described in Section 8.4.3.[2] When an action potential depolarizes the presynaptic terminal, a voltage-gated channel in the membrane is activated that allows up to four Ca^{+2} to bind to a binding protein, R, on the outside of the cell membrane. When totally bound, the protein joined by four Ca^{+2}, P, moves to the interior of the cell membrane, where it binds with a vesicle, V. A carrier, C, is then joined with PV, forming the bound carrier W. This reaction releases the four Ca^{+2} and the binding protein R. The bound carrier W then moves to the outside of the cell membrane through the opened voltage-gated channel, where vesicle releases n packets of the neurotransmitter N. The overall reaction is given by

$$
\begin{aligned}
&4Ca_o^{+2} + R_o \xrightarrow{B_1} P_o \underset{B_{-2}}{\overset{B_2}{\rightleftharpoons}} P_i \\
&P_i + V_i \xrightarrow{B_3} P_i V_i \\
&C_i + P_i V_i \xrightarrow{B_4} W_i + 4Ca_o^{+2} + R_i \\
&W_i \underset{B_{-5}}{\overset{B_5}{\rightleftharpoons}} W_o \xrightarrow{B_6} V_o + C_o \\
&V_o \xrightarrow{B_7} nN \\
&R_i \xrightarrow{B_8} R_o \\
&C_o \xrightarrow{B_9} C_i
\end{aligned}
\tag{12.53}
$$

where the subscript i and o are the inside and outside. Figure 12.39 shows a model of the four stages of the binding protein with Ca^{+2}, which are described by the following equations.

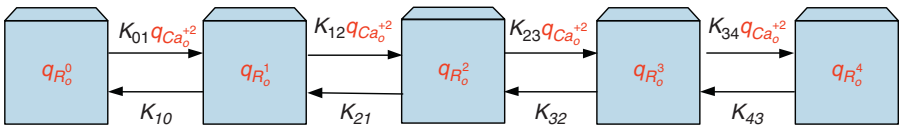

FIGURE 12.39 Carrier-mediated transport of calcium ions into the presynaptic terminal that initiates the movement of the neurotransmitter out of the cell.

[2]A more complex model is given in Section 7.1.3 of Keener and Sneyd that involves probabilistic considerations.

$$
\begin{aligned}
\dot{q}_{Ca_0^{+2}} &= J_{Ca^{+2}} + K_{10}q_{R_o^1} + K_{21}q_{R_o^2} + K_{32}q_{R_o^3} + K_{43}q_{R_o^4} \\
&\quad -K_{01}q_{Ca_0^{+2}}q_{R_o^0} - K_{12}q_{Ca_0^{+2}}q_{R_o^1} - K_{23}q_{Ca_0^{+2}}q_{R_o^2} - K_{34}q_{Ca_0^{+2}}q_{R_o^3} \\
\dot{q}_{R_o^0} &= B_8 q_{R_i} + K_{10}q_{R_o^1} - K_{01}q_{Ca_0^{+2}}q_{R_o^0} \\
\dot{q}_{R_o^1} &= K_{21}q_{R_o^2} + K_{01}q_{Ca_0^{+2}}q_{R_o^0} - K_{10}q_{R_o^1} - K_{12}q_{Ca_0^{+2}}q_{R_o^1} \\
\dot{q}_{R_o^2} &= K_{32}q_{R_o^3} + K_{12}q_{Ca_o^{+2}}q_{R_o^1} - K_{21}q_{R_o^2} - K_{23}q_{Ca_o^{+2}}q_{R_o^2} \\
\dot{q}_{R_o^3} &= K_{43}q_{R_o^4} + K_{23}q_{Ca_o^{+2}}q_{R_o^2} - K_{32}q_{R_o^3} - K_{34}q_{Ca_o^{+2}}q_{R_o^3} \\
\dot{q}_{R_o^4} &= K_{34}q_{Ca_o^{+2}}q_{R_o^3} - K_{43}q_{R_o^4} - B_1 q_{R_o^4}
\end{aligned}
\tag{12.54}
$$

where R_o^i has i Ca_o^{+2} bound to it, the transfer rates, $K_{i,j}$, are functions of membrane voltage, and $J_{Ca^{+2}}$ is the flow of Ca^{+2} out of the cell. Here, we assume that the quantity of Ca^{+2} is constant and given by $\gamma = q_{Ca_i^{+2}} + q_{Ca_o^{+2}} - q_{R_o^0} - q_{R_o^1} - q_{R_o^2} - q_{R_o^3} - q_{R_o^4}$. The flow $J_{Ca^{+2}}$ is due to an active pump that keeps the concentration of Ca^{+2} in the cytosol low, while the concentration outside the cell is very high. One can imagine a similar process for the $J_{Ca^{+2}}$ active pump as given for the *Na-K* pump described in Section 8.4.4. The transfer rates are zero at resting potential and increase as the membrane depolarizes (Keener and Sneyd use exponential functions for the transfer rates). Next, we have

$$
\begin{aligned}
\dot{q}_{P_o} &= B_1 q_{R_o^4} + B_{-2}q_{P_i} - B_2 q_{P_o} \\
\dot{q}_{P_i} &= B_2 q_{P_o} - B_{-2}q_{P_i} - B_3 q_{P_i} q_{V_i} \\
\dot{q}_{V_i} &= J_{V_i} - B_3 q_{P_i} q_{V_i} \\
\dot{q}_{V_o} &= B_6 q_{W_o} - B_7 q_{V_o} \\
\dot{q}_{W_i} &= B_4 q_{C_i} q_{P_i V_i} + B_{-5} q_{W_o} - B_5 q_{W_i} \\
\dot{q}_{W_o} &= B_5 q_{W_i} - B_{-5} q_{W_o} - B_6 q_{W_o} \\
\dot{q}_{C_i} &= B_9 q_{C_o} - B_4 q_{C_i} q_{P_i V_i} \\
\dot{q}_{C_o} &= B_6 q_{W_o} - B_9 q_{C_o} \\
\dot{q}_{N_o} &= n B_7 q_{V_o}
\end{aligned}
\tag{12.55}
$$

where J_{V_i} is the rate of the creation of new vesicles.

It should be noted that the vesicles absorbed into the cell membrane during the movement of the neurotransmitter out of the cell, after a period of time, leave the cell membrane and reform in the cytosol with the same characteristics as before. The vesicle then synthesizes the neurotransmitter using enzyme proteins in its membrane using ATP from the mitochondria. For example, ACh is resupplied inside the vesicle using a carrier-mediated enzyme choline acetyltransferase that binds acetyl coenzyme and choline similar to the reaction described in Section 8.4.3. The entire process from receipt of the action potential at the presynaptic terminal to release of the neurotransmitter takes less than 1 ms.

12.8.2 Postsynaptic Neurons

Once the neurotransmitter is released from the presynaptic neuron, it diffuses across the synaptic gap and binds to the receptors on the postsynaptic neuron's dendrite. Once bound to the dendrite, the neurotransmitter moves into the cytosol by carrier-mediated transport, where once in the cytosol, an ion channel opens. If the neurotransmitter is excitatory, Na^+ flows into the open channel, and the membrane depolarizes. If the neurotransmitter is inhibitory, Cl^- flows into the open channel, and the membrane hyperpolarizes. This process takes less than 1 ms. The change in membrane potential lasts up to 15 ms due to the capacitive nature of the membrane, thus allowing for temporal summation of all the neurotransmitter secreted by the many presynaptic terminals.

Consider the neurotransmitter ACh and its carrier-mediated transport into the cytosol of the postsynaptic neuron. ACh binds to the enzyme choline acetyltransferase, C, that transports it across the membrane, allowing it to pass into the cytosol. Using the model illustrated in Figure 8.21, we have

$$\begin{aligned} &ACh_0 + C_0 \xrightarrow{K_1} P_o \underset{K_2}{\overset{K_2}{\rightleftharpoons}} P_i \xrightarrow{K_3} ACh_i + C_i \\ &ACh_i \xrightarrow{K_4} A_i + Ch_i \\ &C_o \underset{K_2}{\overset{K_2}{\rightleftharpoons}} C_i \end{aligned} \tag{12.56}$$

where P is the bound substrate and carrier complex, A is acetyl coenzyme A, and Ch is choline. As before, i and o subscripts refer to the inside and outside of the cell. We assume that A and Ch are moved from the cytosol into the synaptic gap by diffusion and that the flow of ACh into the synaptic gap from the presynaptic neuron is given by N_o (now called ACh_o) from Eq. (12.55). The equations that describe this system are given by

$$\begin{aligned} \dot{q}_{ACh_o} &= -K_1 q_{ACh_o} q_{C_o} + nB_7 q_{V_o} \\ \dot{q}_{C_o} &= -K_1 q_{ACh_o} q_{C_o} + K_2 q_{C_i} - K_2 q_{C_o} \\ \dot{q}_{P_o} &= K_1 q_{ACh_o} q_{C_o} + K_2 q_{P_i} - K_2 q_{P_o} \\ \dot{q}_{P_i} &= K_2 q_{P_o} - K_1 q_{P_i} \\ \dot{q}_{ACh_i} &= K_1 q_{P_i} - K_4 q_{ACh_i} \\ \dot{q}_{C_i} &= K_1 q_{P_i} + K_2 q_{C_o} - K_2 q_{C_i} \\ \dot{q}_{A_i} &= K_4 q_{ACh_i} - D_A q_{A_i} \\ \dot{q}_{Ch_i} &= K_4 q_{ACh_i} - D_{Ch} q_{Ch_i} \end{aligned} \tag{12.57}$$

To capture the change in conductance as a function of ACh_i, and its impact on the membrane potential, we introduce another channel in the dendritic membrane section, as shown in Figure 12.40, where the stimulus current, I_s, from the neurotransmitter is

$$I_s = \frac{V_m - V_{TH}}{R(ACh_i)} \tag{12.58}$$

where $R(ACh_i)$ is the channel resistance that depends on the quantity of ACh_i.

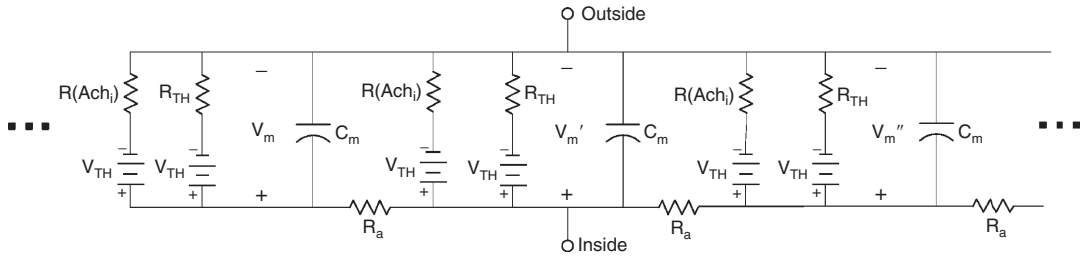

FIGURE 12.40 Equivalent circuit of series of dendritic membrane sections that includes a neurotransmitter channel. Each section is connected together with an axial resistance, R_a.

A complete model of the neuron can be constructed by including as many dendritic branches as needed, each described using Figure 12.17 and modeled by

$$\begin{aligned}&\ldots + C_m\frac{dV_m}{dt} + \frac{(V_m - V_{TH})}{R(ACh_i)} + \frac{(V_m - V_{TH})}{R_{TH}} + \frac{(V_m - V'_m)}{R_a}\\ &+C_m\frac{dV'_m}{dt} + \frac{(V'_m - V_{TH})}{R(ACh_i)} + \frac{(V'_m - V_{TH})}{R_{TH}} + \frac{(V'_m - V''_m)}{R_a} + \ldots\end{aligned} \tag{12.59}$$

Although this chapter has focused on the neuron, it is important to note that numerous other cells have action potentials that involve signaling or triggering. Many of the principles discussed in this chapter apply to these other cells as well, but the action potential defining equations are different. For example, the cardiac action potential can be defined with a DiFranceso-Noble, Luo-Rudy, or other models instead of a Hodgkin-Huxley model of the neuron.

12.9 EXERCISES

1. Assume a membrane is permeable to only Ca^{+2}. (a) Derive the expression for the flow of Ca^{+2}. (b) Find the Nernst potential for Ca^{+2}.
2. Assume that a membrane is permeable to Ca^{+2} and Cl^{-} but not to a large cation R^{+}. The inside concentrations are $[RCl] = 100$ mM and $[CaCl_2] = 200$ mM, and the outside concentration is $[CaCl_2] = 300$ mM. (a) Derive the Donnan equilibrium. (b) Find the steady-state concentration for Ca^{+2}.
3. Assume that a membrane is permeable to Ca^{+2} and Cl^{-}. The initial concentrations on the inside are different from the outside, and these are the only ions in the solution. (a) Write an equation for J_{Ca} and J_{Cl}. (b) Write an expression for the relationship between J_{Ca} and J_{Cl}. (c) Find the steady-state voltage. (d) Find the relationship between the voltage across the membrane and $[CaCl_2]$ before steady-state.
4. Assume that a membrane is permeable to only ion R^{+3}. The inside concentration is $[RCl_3] = 2$ mM, and the outside concentration is $[RCl_3] = 1.4$ mM. (a) Write an expression for the flow of R^{+3}. (b) Derive the Nernst potential for R^{+3} at steady-state.

5. Derive the Goldman equation for a membrane in which Na^+, K^+, and Cl^- are the only permeable ions.
6. Calculate V_m for the frog skeletal muscle at room temperature.
7. The following steady-state concentrations and permeabilities are given for a red blood cell membrane.

Ion	Cytoplasm (mM)	Extracellular Fluid (mM)	Ratio of Permeabilities
K^+	140	4	1.0
Na^+	11	145	0.54
Cl^-	80	116	0.21

(a) Find the Nernst potential for each ion. (b) What is the resting potential predicted by the Goldman equation?

8. The following steady-state concentrations and permeabilities are given for a skeletal muscle membrane.

Ion	Cytoplasm (mM)	Extracellular Fluid (mM)	Ratio of Permeabilities
K^+	150	5	0.1
Na^+	12	145	0.001
Cl^-	4	116	1.0

(a) Find the Nernst potential for each ion. (b) What is the resting potential predicted by the Goldman equation?

9. The following steady-state concentrations and permeabilities are given for a membrane.

Ion	Cytoplasm (mM)	Extracellular Fluid (mM)	Ratio of Permeabilities
K^+	140	2.5	1.0
Na^+	13	110	0.019
Cl^-	3	90	0.381

(a) Find the Nernst potential for K^+. (b) What is the resting potential predicted by the Goldman equation? (c) Explain whether space charge neutrality is satisfied. (d) Explain why the steady-state membrane potential does not equal zero.

10. A membrane has the following concentrations and permeabilities.

Ion	Cytoplasm (mM)	Extracellular Fluid (mM)	Ratio of Permeabilities
K^+	?	4	?
Na^+	41	276	0.017
Cl^-	52	340	0.412

The resting potential of the membrane is -52 mV at room temperature. Find the K^+ cytoplasm concentration.

11. The following steady-state concentrations and permeabilities are given for a membrane. Note that A^+ is not permeable.

Ion	Cytoplasm (mM)	Extracellular Fluid (mM)	Ratio of Permeabilities
K^+	136	15	1.0
Na^+	19	155	0.019
Cl^-	78	112	0.381
A^+	64	12	—

Continued

(a) Find the Nernst potential for Cl^-. (b) What is the resting potential predicted by the Goldman equation? (c) Explain whether space charge neutrality is satisfied. (d) Explain why the steady-state membrane potential does not equal zero. (e) Explain why the resting potential does not equal the Nernst potential of any of the ions.

12. A membrane is permeable to K^+ and Cl^- but not to cation R^+. Find the steady-state equilibrium concentrations for the following system's initial conditions.

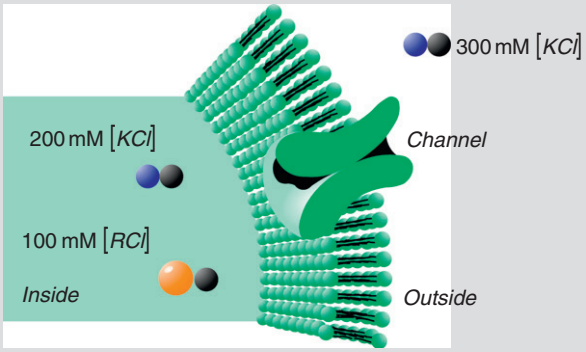

13. A membrane is permeable to B^{+3} and Cl^- but not to a large cation R^+. The following initial concentrations are given.

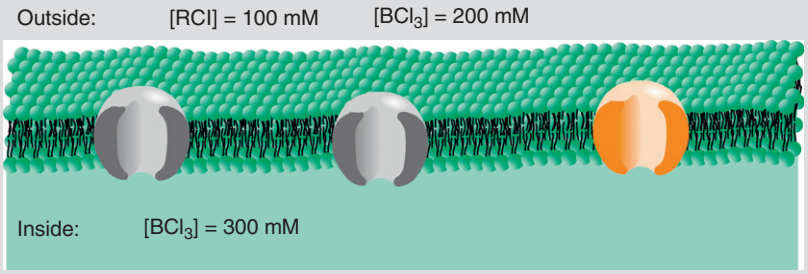

(a) Derive the Donnan equilibrium. (b) Find the steady-state concentration for B^{+3}.

14. The following membrane is permeable to Ca^{+2} and Cl^-. (a) Write expressions for the flow of Ca^{+2} and Cl^- ions. (b) Write an expression for the relationship between J_{Ca} and J_{Cl}. (c) Find the steady-state voltage. (d) Find the relationship between voltage across the membrane and the concentration of $CaCl_2$ before steady-state is reached.

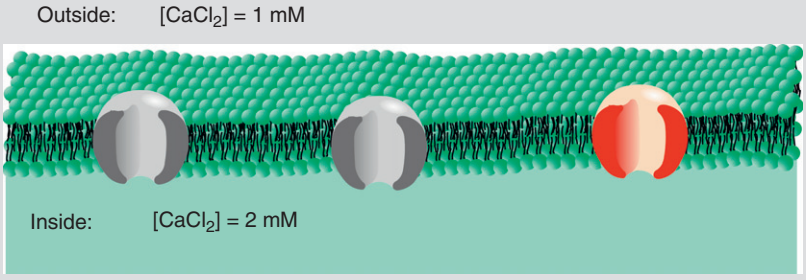

15. The following membrane has an active Ca^{+2} pump. Assume that the membrane is permeable to both Ca^{+2} and Cl^{-}, and the Ca^{+2} pump flow is J_p. The width of the membrane is δ. Find the pump flow as a function of $\left[Ca^{+2}\right]$.

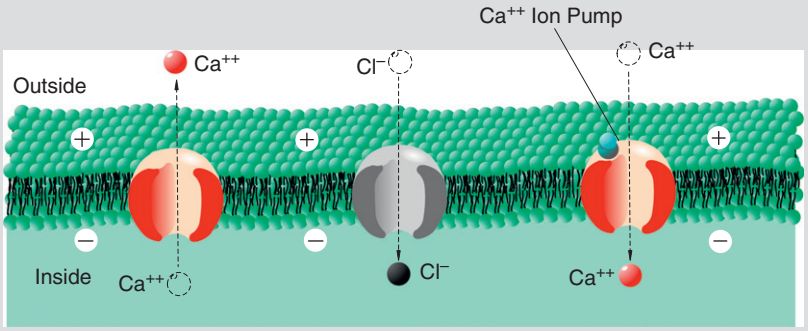

16. The membrane shown is permeable to K^{+} and Cl^{-}. The active pump transports K^{+} from the outside to the inside of the cell. The width of the membrane is δ.
(a) Write an equation for the flow of each ion. (b) Find the flows at steady-state. (c) Find the pump flow as a function of $\left([K^{+}]_i - [K^{+}]_o\right)$. (d) Qualitatively describe the ion concentration on each side of the membrane.

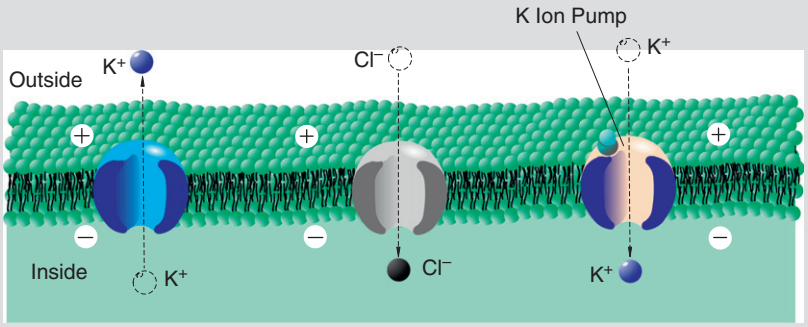

17. The following membrane is given with two active pumps. Assume that the membrane is permeable to $Na^{+}, K^{+},$ and Cl^{-} and $J_p(K) = J_p(Na) = J_p$. The width of the membrane is δ. Solve for the quantity $\left([Cl^{-}]_i - [Cl^{-}]_o\right)$ as a function of J_p.

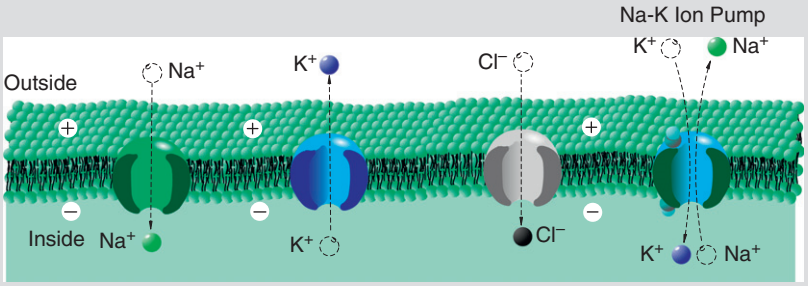

Continued

18. The following steady-state concentrations and permeabilities are given for a membrane. Note that A^+ is not permeable. The ion channel resistances are $R_K = 1.7\ \text{k}\Omega, R_{Na} = 9.09\ \text{k}\Omega,$ and $R_{Cl} = 3.125\ \text{k}\Omega$.

Ion	Cytoplasm (mM)	Extracellular Fluid (mM)	Ratio of Permeabilities
K^+	168	6	1.0
Na^+	50	337	0.019
Cl^-	41	340	0.381
A^+	64	12	—

(a) Find the Nernst potential for each ion. (b) Draw a circuit model for this membrane. (Hint: See Figure 12.13.) (c) Find the membrane resting potential using the circuit in part (b). (d) Find the Thevenin's equivalent circuit for the circuit in part (b).

19. Suppose the membrane in Figure 12.13 is given with $R_K = 0.1\ \text{k}\Omega, R_{Na} = 2\ \text{k}\Omega, R_{Cl} = 0.25\ \text{k}\Omega,$ $E_K = -74\ \text{mV}, E_{Na} = 55\ \text{mV},$ and $E_{Cl} = -68\ \text{mV}$. (a) Find V_m. (b) Find the Thevenin's equivalent circuit.

20. Suppose a membrane has an active *Na-K* pump with $R_K = 0.1\ \text{k}\Omega, R_{Na} = 2\ \text{k}\Omega, R_{Cl} = 0.25\ \text{k}\Omega,$ $E_K = -74\ \text{mV}, E_{Na} = 55\ \text{mV},$ and $E_{Cl} = -68\ \text{mV},$ as shown in Figure 12.14. Find I_{Na} and I_K for the active pump.

21. The following steady-state concentrations and permeabilities are given for a membrane. Note that A^+ is not permeable.

Ion	Cytoplasm (mM)	Extracellular Fluid (mM)	Ratio of Permeabilities
K^+	140	2.5	1.0
Na^+	13	110	0.019
Cl^-	3	90	0.381
A^+	64	12	—

(a) If $R_K = 1.7\ \text{k}\Omega$ and $\text{R}_{\text{Cl}} = 3.125\ \text{k}\Omega,$ then find R_{Na}. (b) Find the Thevenin's equivalent circuit model.

22. Suppose that a membrane that has an active *Na-K* pump with $R_K = 0.1\ \text{k}\Omega,$ $R_{Na} = 2\ \text{k}\Omega,$ $R_{Cl} = 0.25\ \text{k}\Omega,$ $E_K = -74\ \text{mV},$ $E_{Na} = 55\ \text{mV},$ $E_{Cl} = -68\ \text{mV},$ and $C_m = 1\ \mu\text{F},$ as shown in Figure 12.15, is stimulated by a current pulse of 10 μA for 6 ms. (a) Find V_m. (b) Find the capacitive current. (c) Calculate the size of the current pulse applied at 6 ms for 1 ms, necessary to raise V_m to -40 mV. (d) If the threshold voltage is -40 mV and the stimulus is applied as in part (c), then explain whether an action potential occurs.

23. Suppose that a membrane that has an active *Na-K* pump with $R_K = 2.727\ \text{k}\Omega,$ $R_{Na} = 94.34\ \text{k}\Omega,$ $R_{Cl} = 3.33\ \text{k}\Omega,$ $E_K = -72\ \text{mV},$ $E_{Na} = 55\ \text{mV},$ $E_{Cl} = -49.5\ \text{mV},$ and $C_m = 1\mu\text{F},$ shown in Figure 12.15, is stimulated by a current pulse of 13 μA for 6 ms. Find (a) V_m, (b) I_K, and (c) the capacitive current.

24. Suppose a membrane has an active *Na-K* pump with $R_K = 1.75\ \text{k}\Omega,$ $R_{Na} = 9.09\ \text{k}\Omega,$ $R_{Cl} = 3.125\ \text{k}\Omega,$ $E_K = -85.9\ \text{mV},$ $E_{Na} = 54.6\ \text{mV},$ $E_{Cl} = -9.4\ \text{mV},$ and $C_m = 1\mu\text{F}$ as shown in Figure 12.15. (a) Find the predicted resting membrane potential. (b) Find V_m if a small subthreshold current pulse is used to stimulate the membrane.

25. Suppose a membrane has an active *Na-K* pump with $R_K = 2.727\ \text{k}\Omega, R_{Na} = 94.34\ \text{k}\Omega, R_{Cl} = 3.33\ \text{k}\Omega,\ E_K = -72\ \text{mV}, E_{Na} = 55\ \text{mV}, E_{Cl} = -49.5\ \text{mV},$ and $C_m = 1\ \mu\text{F}$, as shown in Figure 12.15. Design a stimulus that will drive V_m to threshold at 3 ms. Assume that the threshold potential is -40 mV. (a) Find the current pulse magnitude and duration. (b) Find and sketch V_m.

26. Suppose a current pulse of 20 μA is passed through the membrane of a squid giant axon. The Hodgkin-Huxley parameter values for the squid giant axon are $G_l = \dfrac{1}{R_l} = 0.3 \times 10^{-3}\ \text{S}, \bar{G}_K = 36 \times 10^{-3}\ \text{S}, \bar{G}_{Na} = 120 \times 10^{-3}\ \text{S}, E_K = -72 \times 10^{-3}\ \text{V}, E_l = -49.4 \times 10^{-3}\ \text{V}, E_{Na} = 55 \times 10^{-3}\ \text{V}$ and $C_m = 1 \times 10^{-6}\ \text{F}$. Simulate the action potential. Plot (a) V_m, G_{Na}, and G_K versus time, (b) V_m, n, m, and h versus time, and (c) V_m, I_{Na}, I_K, I_c, and I_l versus time.

27. Suppose a current pulse of 20 μA is passed through an axon membrane. The parameter values for the axon are $G_l = \dfrac{1}{R_l} = 0.3 \times 10^{-3}\ \text{S}, \bar{G}_K = 36 \times 10^{-3}\ \text{S}, E_K = -12 \times 10^{-3}\ \text{V}, E_l = 10.6 \times 10^{-3}\ \text{V}, E_{Na} = 115 \times 10^{-3}\ \text{V}$, and $C_m = 1 \times 10^{-6}\ \text{F}$. Assume that Eqs. (12.41) to (12.48) describe the axon. Simulate the action potential. Plot (a) V_m, G_{Na}, and G_K versus time, (b) V_m, n, m, and h versus time, and (c) V_m, I_{Na}, I_K, I_c, and I_l versus time.

28. This exercise examines the effect of the threshold potential on an action potential for the squid giant axon. The Hodgkin-Huxley parameter values for the squid giant axon are $G_l = \dfrac{1}{R_l} = 0.3 \times 10^{-3}\ \text{S}, \bar{G}_K = 36 \times 10^{-3}\ \text{S}, \bar{G}_{Na} = 120 \times 10^{-3}\ \text{S}, E_K = -72 \times 10^{-3}\ \text{V}, E_l = -49.4 \times 10^{-3}\ \text{V}, E_{Na} = 55 \times 10^{-3}\ \text{V}$, and $C_m = 1 \times 10^{-6}\ \text{F}$. (a) Suppose a current pulse of -10 μA, which hyperpolarizes the membrane, is passed through the membrane of a squid giant axon for a very long time. At time $t = 0$, the current pulse is removed. Simulate the resultant action potential. (b) The value of the threshold potential is defined as when $I_{Na} > I_K + I_l$. Changes in threshold potential can be easily implemented by changing the value of 25 in the equation for α_m to a lower value. Suppose the value of 25 is changed to 10 in the equation defining α_m and a current pulse of -10 μA (hyperpolarizes the membrane) is passed through the membrane of a squid giant axon for a very long time. At time $t = 0$, the current pulse is removed. Simulate the resultant action potential.

29. Simulate the plots shown in Figures 12.20 to 12.22 in the voltage clamp mode.

30. Select an input current waveform necessary to investigate the refractory period that follows an action potential. (Hint: Use a two-pulse current input.) What is the minimum refractory period? If the second pulse is applied before the minimum refractory period, how much larger is the stimulus magnitude that is needed to generate an action potential?

31. Explain whether the following circuit allows the investigator to conduct a voltage clamp experiment. The unmyelinated axon is sealed at both ends. A silver wire is inserted inside the axon that eliminates R_a. Clearly state any assumptions.

Continued

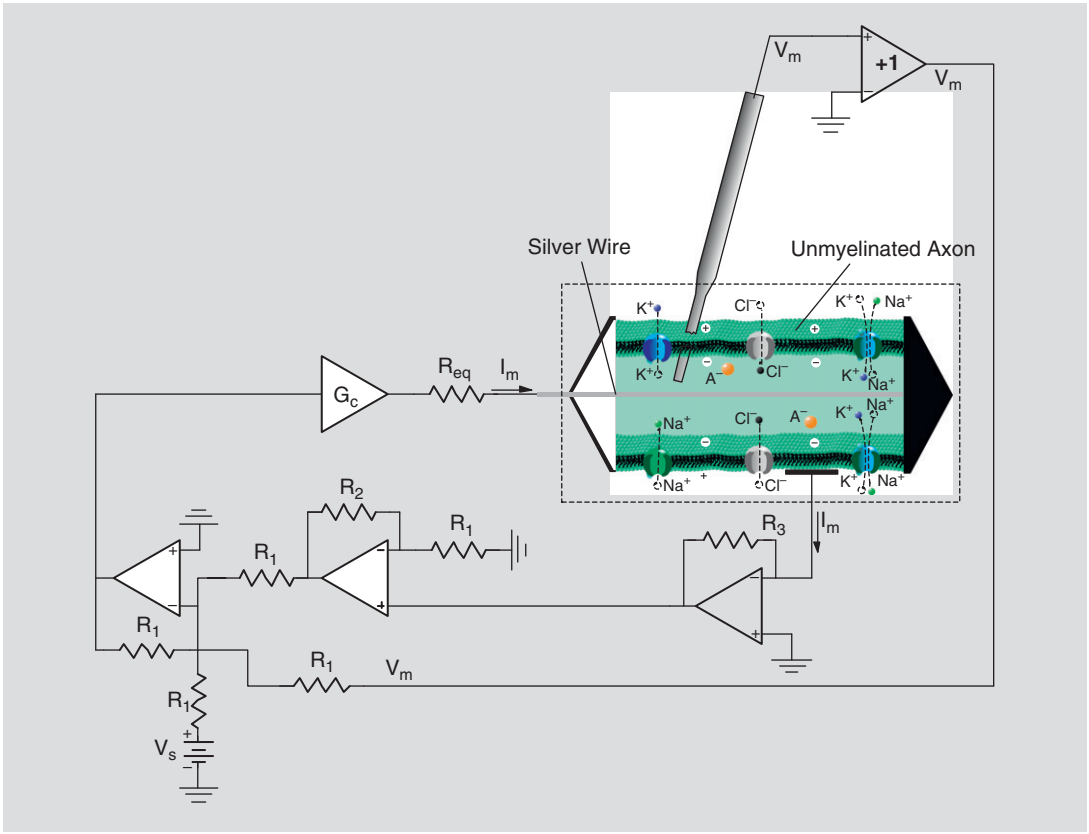

References

[1] T.D. Coates, Neural Interfacing: Forging the Human-Machine Connection, Morgan & Claypool Publishers, LaPorte, Colorado, 2008.
[2] J. Keener, J. Sneyd, Mathematical Physiology, Springer, New York, 1998.
[3] F. Rodriguez Campos, J.D. Enderle, Porting Genesis to SIMULINK, in: Proceedings of the 30th IEEE EMBS Annual International Conference, September 2–5, 2004.
[4] J.C. Sanchez, J.C. Principe, Brain-Machine Interface Engineering, Morgan & Claypool Publishers, LaPorte, Colorado, 2007.

Suggested Readings

A.T. Bahill, Bioengineering: Biomedical, Medical and Clinical Engineering, Prentice-Hall, Inc., Englewood Cliffs, NJ, 1981.
J.D. Bronzino, The Biomedical Engineering Handbook, CRC Press, Inc., Boca Raton, FL, 2000.
J.M. Bower, D. Beeman, The Book of Genesis: Exploring Realistic Neural Models with the General Neural Simulation System, Springer-Verlag, New York, 1998.
S. Deutsch, A. Deutsch, Understanding the Nervous System—An Engineering Perspective, IEEE Press, New York, 1993.
D. DiFrancesco, D. Noble, A model of cardiac electrical activity incorporating ionic pumps and concentration changes, Philos. Trans. R. Soc. Lond. B Biol. Sci. 307 (1985) 307–353.

J.D. Enderle, Neural Control of Saccades, in: J. Hyönä, D. Munoz, W. Heide, R. Radach (Eds.), The Brain's Eyes: Neurobiological and Clinical Aspects to Oculomotor Research, Progress in Brain Research, vol. 140, Elsevier, Amsterdam, 2002, pp. 21–50.

J.F. Fulton, H. Cushing, A bibliographical study of the Galvani and Aldini writings on animal electricity, Ann. Sci. 1 (1936) 239–268.

A.C. Guyton, J.E. Hall, Textbook on Medical Physiology, ninth ed., W.B. Saunders Co., Philadelphia, 1995.

B. Hille, Ionic Channels of Excitable Membranes, second ed., Sunderland, Massachusetts, 1992.

A. Hodgkin, A. Huxley, B. Katz, Measurement of current-voltage relations in the membrane of the giant axon of Loligo, J. Physiol. (London) 116 (1952) 424–448.

A. Hodgkin, A. Huxley, Currents carried by sodium and potassium ions through the membrane of the giant axon of Loligo, J. Physiol. (London) 116 (1952) 449–472.

A. Hodgkin, A. Huxley, The components of membrane conductance in the giant axon of Loligo, J. Physiol. (London) 116 (1952) 473–496.

A. Hodgkin, A. Huxley, The dual effect of membrane potential on sodium conductance in the giant axon of Loligo, J. Physiol. (London) 116 (1952) 497–506.

A. Hodgkin, A. Huxley, A quantitative description of membrane current and its application to conduction and excitation in nerve, J. Physiol. (London) 117 (1952) 500–544.

E.R. Kandel, J.H. Schwartz, T.M. Jessell, Principles of Neural Science, fifth ed., McGraw-Hill, New York, 2000.

C. Koch, I. Segev, Methods in Neuronal Modeling, From Ions to Networks, MIT Press, Cambridge, Massachusetts, 1998.

C. Luo, Y. Rudy, A dynamic model of the cardiac ventricular action potential: I. Simulations of ionic currents and concentration changes, Circ. Res. 74 (1994) 1071.

G.G. Matthews, Cellular Physiology of Nerve and Muscle, Blackwell Scientific Publications, Boston, 1991.

W. Nernst, Die elektromotorishe Wirksamkeit der Jonen, Z. Physik. Chem. 4 (1889) 129–188.

R. Plonsey, R.C. Barr, Bioelectricity: A Quantitative Approach, Plenum Press, New York, 1982.

R. Northrop, Introduction to Dynamic Modeling of Neurosensory Systems, CRC Press, Boca Raton, 2001.

J. Rinzel, Electrical excitability of cells, theory and experiment: Review of the Hodgkin-Huxley foundation and an update, in: M. Mangel (Ed.), Bull. Math. Biology: Classics of Theoretical Biology, vol. 52, 1990, , pp. 5–23.

J.V. Tranquillo, Quantitative Neurophysiology, Morgan & Claypool Publishers, LaPorte, Colorado, 2008.